
CONJUGATE GRADIENT METHOD FOR GENERATIVE ADVERSARIAL NETWORKS

A PREPRINT

Hiroki Naganuma

Mila and DIRO,

Université de Montréal

naganuma.hiroki@mila.quebec

Hideaki Iiduka

Department of Computer Science,

Meiji University

iiduka@cs.meiji.ac.jp

ABSTRACT

While the generative model has many advantages, it is not feasible to calculate the Jensen–Shannon divergence of the density function of the data and the density function of the model of deep neural networks; for this reason, various alternative approaches have been developed. Generative adversarial networks (GANs) can be used to formulate this problem as a discriminative problem with two models, a generator and a discriminator whose learning can be formulated in the context of game theory and the local Nash equilibrium. Since this optimization is more difficult than minimization of a single objective function, we propose to apply the conjugate gradient method to solve the local Nash equilibrium problem in GANs. We give a proof and convergence analysis under mild assumptions showing that the proposed method converges to a local Nash equilibrium with three different learning-rate schedules including a constant learning rate. Furthermore, we demonstrate the convergence of a simple toy problem to a local Nash equilibrium and compare the proposed method with other optimization methods in experiments using real-world data, finding that the proposed method outperforms stochastic gradient descent (SGD) and momentum SGD.

Keywords Optimization · Deep Learning · Generative Adversarial Networks (GANs)

1 Introduction

Generative models that estimate the observed data’s probability distribution play important roles in machine learning. Discriminative models, which classify data by learning a classification function based on a suitable combination of attributes of the observed data, do not model anything about the process or probability of generating the given data. Generative model training involves minimizing the Jensen–Shannon divergence between the density function of the data and the density function of the generative model. However, as this is computationally infeasible, the generative adversarial networks (GANs) concept [Goo+14] has been proposed to turn the training into a discrimination problem using a discriminator network and a generator network.

Since the advent of GANs in 2014, research has rapidly progressed to include deep convolutional (DC) GAN [RMC15], which is specialized to image recognition; CycleGAN [Zhu+17] and StyleGAN [KLA19], which change the styles of images; BigGAN [BDS18], which increases the resolution of images; StackGAN [Zha+17], which generates images from the text; and a wide range of other applications, such as image inpainting [Pat+16], video frame completion [Mey+15], font generation [HAU19], and speech [DMP18] and text generation [FGD18]. Besides these applications, GANs are also being used to generate data for expanding and augmenting datasets used in medical image segmentation tasks [San+19], and GANs-based methods are being adapted for domain generalization [San+19] to coordinate models across different domains.

One way of training GANs is to solve a Nash equilibrium problem [Nas51] with two players, a discriminator that minimizes the synthetic-real discrimination error and a generator that maximizes this error.

Two useful algorithms were presented in [Heu+17] based on two time-scale update rules for finding a local Nash equilibrium in GANs. One algorithm is based on stochastic gradient descent (SGD), and the other is adaptive moment

Table 1: Convergence rates of our algorithms with constant and diminishing learning rates

		Constant learning rate ($a_n = a, b_n = b$)	Diminishing learning rate ($a_n = n^{-1/2}, b_n = n^{-1/2}$)	Diminishing learning rate ($a_n = n^{-\eta_a}, b_n = n^{-\eta_b}$)
SGD	Generator	$\mathcal{O}(N^{-1}) + C_1^G a$	$\mathcal{O}(N^{-1/2})$	$\mathcal{O}(N^{-\min\{\eta_a, 1-\eta_a\}})$
	Discriminator	$\mathcal{O}(N^{-1}) + C_1^D b$	$\mathcal{O}(N^{-1/2})$	$\mathcal{O}(N^{-\min\{\eta_b, 1-\eta_b\}})$
Momentum	Generator	$\mathcal{O}(N^{-1}) + C_1^G a + C_2^G \beta^G$	$\mathcal{O}(N^{-1/2})$	$\mathcal{O}(N^{-\min\{\eta_a, 1-\eta_a\}})$
	Discriminator	$\mathcal{O}(N^{-1}) + C_1^D b + C_2^D \beta^D$	$\mathcal{O}(N^{-1/2})$	$\mathcal{O}(N^{-\min\{\eta_b, 1-\eta_b\}})$
CG	Generator	$\mathcal{O}(N^{-1}) + C_1^G a + C_2^G \beta^G$	$\mathcal{O}(N^{-1/2})$	$\mathcal{O}(N^{-\min\{\eta_a, 1-\eta_a\}})$
	Discriminator	$\mathcal{O}(N^{-1}) + C_1^D b + C_2^D \beta^D$	$\mathcal{O}(N^{-1/2})$	$\mathcal{O}(N^{-\min\{\eta_b, 1-\eta_b\}})$

C_i^G and C_i^D ($i = 1, 2$) are positive constants independent of learning rates a and b and number of iterations N . β^G and β^D are upper bounds of the CG parameter β_n^G and β_n^D , respectively (see Assumption 3.1(C2) for details). η_a and η_b satisfy $1/2 < \eta_b < \eta_a < 1$. The convergence rate is measured as the expectation of the variational inequality (see, e.g., (9) and (10)), where we assume that the stochastic gradient errors are zero. See Theorems 3.1 and 3.2 for detailed convergence analyses.

estimation (Adam). The two algorithms converge almost surely to stationary local Nash equilibria when they use *diminishing* learning rates [Heu+17, (A2)], [Heu+17, Theorems 1 and 2]. Meanwhile, numerical results [Heu+17] have shown that the two algorithms also perform well when they use *constant* learning rates.

1.1 Motivation

We have two motivations that are related to the results in [Heu+17].

- The first is to identify whether optimization algorithms based on two time-scale update rules with *constant* learning rates can, in theory, be applied to local Nash equilibrium problems in GANs.

This motivation is related to bridging the gap between theory and practice for optimization algorithms with two time-scale update rules [Heu+17].

- The second motivation is to identify whether *conjugate gradient* (CG)-type algorithms, which use CG directions to search for minimizers of the observed loss functions, can in theory and in practice be applied to local Nash equilibrium problems.

Generally, SGD and its variants generate search directions by using the gradients of loss functions at the current approximation point. One method to accelerate SGD is the conjugate gradient (CG) method [NW06, Chapter 5], [HZ06]. The CG direction is defined by not only the current gradient but also the past search direction (see Section 2.2 for the definition of the CG method). CG-type algorithms were studied as ways to solve minimization problems in neural networks [Møl93; Le+11]. Since the local Nash equilibrium problems considered in this paper are more complicated than the minimization problems in [Møl93; Le+11], it is not guaranteed that the CG-type algorithms in [Møl93; Le+11] can be applied to them. This raises a fascinating issue as to whether or not CG-type algorithms can find stationary local Nash equilibria more stably and faster than the state-of-the-art algorithms for training GANs.

1.2 Contribution of this paper

This paper makes three contributions.

- The first contribution is to propose a CG-type algorithm (Algorithm 1) for solving local Nash equilibrium problems in GANs.

The proposed algorithm uses the CG direction defined by both the current search direction and past search direction, in contrast to the SGD-type and Adam-type algorithms in [Heu+17] that use only stochastic gradient directions. In particular, this allows us to use efficient CG parameters, such as the Fletcher–Reeves (FR) [FR64], Polak–Ribièr–Polyak (PRP) [PR69; Pol69], Hestenes–Stiefel (HS) [HS52], Dai–Yuan (DY) [DY99] formulas, to generate the CG direction. Hence, we expect that the proposed algorithm performs better than the ones using stochastic gradient directions. We also should note that the proposed algorithm includes the SGD-type and momentum-type algorithms (see Table 1 and Sections 3.1.2 and 3.2.2).

- The second contribution is to present convergence and convergence rate analyses of the proposed algorithm with a constant learning rate rule (Theorem 3.1) and a diminishing learning rate rule (Theorem 3.2).

Our results on the convergence rates are summarized in Table 1. We would like to emphasize that the main theoretical contribution is showing convergence as well as the convergence rate of the proposed algorithm with *constant* learning rates (Theorem 3.1 and Table 1), which is in contrast to the previous results for algorithms with diminishing learning rates (see [Heu+17] for training GANs and [KB15; RKK18] for training deep neural networks). The results indicate that the proposed algorithm using a small constant learning rate achieves approximately an $\mathcal{O}(N^{-1})$ convergence rate (Table 1 and (12)), where N denotes the number of iterations. This implies that optimization algorithms with constant learning rates perform well, as evidenced in [Heu+17].

We also analyze the convergence as well as the convergence rate of the proposed algorithm with *diminishing* learning rates (Theorem 3.2 and Table 1). The results indicate that the proposed algorithm using diminishing learning rates $a_n = b_n = n^{-1/2}$ achieves an $\mathcal{O}(N^{-1/2})$ convergence rate (Table 1 and (21)). To guarantee that the proposed algorithm converges almost surely to a stationary local Nash equilibrium, we need to use diminishing learning rates $a_n = n^{-\eta_a}$ and $b_n = n^{-\eta_b}$, where $1/2 < \eta_b < \eta_a < 1$. Accordingly, the algorithm for the generator achieves an $\mathcal{O}(N^{-\min\{\eta_a, 1-\eta_a\}})$ convergence rate, while the one for the discriminator achieves an $\mathcal{O}(N^{-\min\{\eta_b, 1-\eta_b\}})$ convergence rate (Table 1 and (23)).

- The third contribution is to provide experimental results showing convergence to a local Nash equilibrium for the SGD, momentum SGD, and CG-type methods (Figure 1). Furthermore, we demonstrate through numerical experiments that the CG type outperforms the SGD and momentum SGD in terms of convergence in problem settings over an extensive hyperparameter search range (Figures 3 and 4).

Convergence to the Nash equilibrium is demonstrated in numerical experiments using the toy example. To the best of our knowledge, ours is the first experimental result showing convergence to the Nash equilibrium with diminishing learning rates such as the inverse square learning rate. Furthermore, we expanded the experimental setting from the toy example by training generators of SGD, momentum SGD, and seven different CG type on real-world datasets and compared their FID scores, one of the measures used in GANs training. The results show that the CG methods perform better than the other methods, both on average and in terms of best performance.

2 Mathematical Preliminaries

The notation used in this paper is summarized in Table 2.

2.1 Problem formulation

We assume the following conditions [Heu+17, (A1)]:

Assumption 2.1

(A1) $\mathcal{L}_D^{(i)}: \mathbb{R}^\Theta \times \mathbb{R}^W \rightarrow \mathbb{R}$ ($i \in \mathcal{R}$) and $\mathcal{L}_G^{(i)}: \mathbb{R}^\Theta \times \mathbb{R}^W \rightarrow \mathbb{R}$ ($i \in \mathcal{S}$) are continuously differentiable;

(A2) For $\mathbf{w} \in \mathbb{R}^W$, $\mathcal{G}_\mathbf{w}: \mathbb{R}^\Theta \rightarrow \mathbb{R}^\Theta$ is L_1 -Lipschitz continuous.¹ For $\theta \in \mathbb{R}^\Theta$, $\mathcal{D}_\theta: \mathbb{R}^W \rightarrow \mathbb{R}^W$ is L_2 -Lipschitz continuous.

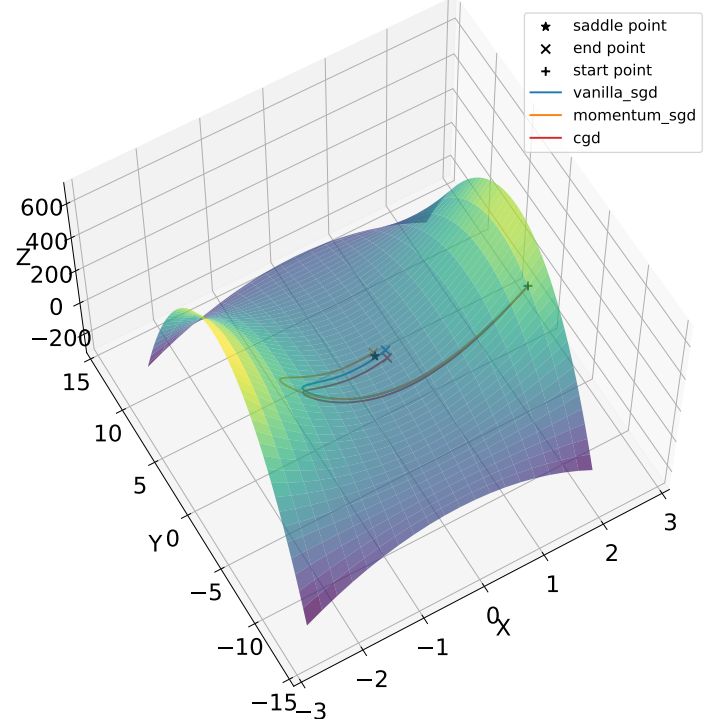


Figure 1. Toy example of minimax optimization using SGD, momentum SGD, and CG method. Objective function: $f(x, y) = (1 + x^2) \cdot (100 - y^2)$. In this figure, we have used inverse square learning rate scheduling for each optimizer.

¹ $A: \mathbb{R}^d \rightarrow \mathbb{R}^d$ is said to be Lipschitz continuous with a Lipschitz constant L (L -Lipschitz continuous) if $\|A(\mathbf{x}) - A(\mathbf{y})\| \leq L\|\mathbf{x} - \mathbf{y}\|$ for all $\mathbf{x}, \mathbf{y} \in \mathbb{R}^d$.

Table 2: Notation List

Notation	Description
\mathbb{N}	The set of all positive integers and zero
$[N]$	$[N] := \{1, 2, \dots, N\} (N \in \mathbb{N} \setminus \{0\})$
$ A $	The number of elements of a set A
\mathbb{R}^d	A d -dimensional Euclidean space with inner product $\langle \cdot, \cdot \rangle$, which induces the norm $\ \cdot\ $
\mathbb{R}_+^d	$\mathbb{R}_+^d := \{\mathbf{x} \in \mathbb{R}^d: x_i \geq 0 (i \in [d])\}$
\mathbb{R}_{++}^d	$\mathbb{R}_{++}^d := \{\mathbf{x} \in \mathbb{R}^d: x_i > 0 (i \in [d])\}$
$\mathbb{E}[X]$	The expectation of a random variable X
$M^{(\mathbf{v})}$	A random variable with respect to a vector \mathbf{v}
\mathcal{R}	The set of real world samples $\mathbf{x}^{(i)}$
\mathcal{S}	The set of synthetic samples $\mathbf{z}^{(i)}$
\mathcal{R}_n	Mini-batch of m real world samples $\mathbf{x}^{(i)}$ at time n
\mathcal{S}_n	Mini-batch of m synthetic samples $\mathbf{z}^{(i)}$ at time n
$\mathcal{L}_D^{(i)}(\boldsymbol{\theta}, \cdot)$	A loss function of discriminator for a fixed $\boldsymbol{\theta} \in \mathbb{R}^\Theta$ and real world sample $\mathbf{x}^{(i)}$
$\mathcal{L}_D(\boldsymbol{\theta}, \cdot)$	A loss function of discriminator for a fixed $\boldsymbol{\theta} \in \mathbb{R}^\Theta$, i.e., $\mathcal{L}_D(\boldsymbol{\theta}, \cdot) := \mathcal{R} ^{-1} \sum_{i \in \mathcal{R}} \mathcal{L}_D^{(i)}(\boldsymbol{\theta}, \cdot)$
$\mathcal{D}_{\boldsymbol{\theta}}(\mathbf{w})$	The gradient of $\mathcal{L}_D^{(i)}(\boldsymbol{\theta}, \cdot)$ for mini-batch \mathcal{R}_n , i.e., $\mathcal{D}_{\boldsymbol{\theta}}(\mathbf{w}) := \sum_{i \in \mathcal{R}_n} \nabla_{\mathbf{w}} \mathcal{L}_D^{(i)}(\boldsymbol{\theta}, \mathbf{w})$
$\mathcal{D}(\boldsymbol{\theta}, \mathbf{w})$	The stochastic gradient of $\mathcal{L}_D^{(i)}(\boldsymbol{\theta}, \cdot)$ for mini-batch \mathcal{R}_n , i.e., $\mathcal{D}(\boldsymbol{\theta}, \mathbf{w}) := m^{-1} \mathcal{D}_{\boldsymbol{\theta}}(\mathbf{w}) + M^{(\mathbf{w})}$
$\mathcal{L}_G^{(i)}(\cdot, \mathbf{w})$	A loss function of generator for a fixed $\mathbf{w} \in \mathbb{R}^W$ and synthetic sample $\mathbf{z}^{(i)}$
$\mathcal{L}_G(\cdot, \mathbf{w})$	A loss function of generator for a fixed $\mathbf{w} \in \mathbb{R}^W$, i.e., $\mathcal{L}_G(\cdot, \mathbf{w}) := \mathcal{S} ^{-1} \sum_{i \in \mathcal{S}} \mathcal{L}_G^{(i)}(\cdot, \mathbf{w})$
$\mathcal{G}_{\mathbf{w}}(\boldsymbol{\theta})$	The gradient of $\mathcal{L}_G^{(i)}(\cdot, \mathbf{w})$ for mini-batch \mathcal{S}_n , i.e., $\mathcal{G}_{\mathbf{w}}(\boldsymbol{\theta}) := \sum_{i \in \mathcal{S}_n} \nabla_{\boldsymbol{\theta}} \mathcal{L}_G^{(i)}(\boldsymbol{\theta}, \mathbf{w})$
$\mathcal{G}(\boldsymbol{\theta}, \mathbf{w})$	The stochastic gradient of $\mathcal{L}_G^{(i)}(\cdot, \mathbf{w})$ for mini-batch \mathcal{S}_n , i.e., $\mathcal{G}(\boldsymbol{\theta}, \mathbf{w}) := m^{-1} \mathcal{G}_{\mathbf{w}}(\boldsymbol{\theta}) + M^{(\boldsymbol{\theta})}$
$\text{LNE}(\mathcal{L}_D, \mathcal{L}_G)$	The set of stationary local Nash equilibria for Nash equilibrium problem for \mathcal{L}_D and \mathcal{L}_G

This paper considers the following local Nash equilibrium problem with two players, a discriminator and a generator [Heu+17]:

Problem 2.1 We would like to find a pair $(\boldsymbol{\theta}^*, \mathbf{w}^*) \in \mathbb{R}^\Theta \times \mathbb{R}^W$ satisfying

$$\nabla_{\mathbf{w}} \mathcal{L}_D(\boldsymbol{\theta}^*, \mathbf{w}^*) = \mathbf{0} \text{ and } \nabla_{\boldsymbol{\theta}} \mathcal{L}_G(\boldsymbol{\theta}^*, \mathbf{w}^*) = \mathbf{0}. \quad (1)$$

A Nash equilibrium $(\boldsymbol{\theta}^*, \mathbf{w}^*) \in \mathbb{R}^\Theta \times \mathbb{R}^W$ [Nas51] defined by

$$\begin{aligned} \mathcal{L}_D(\boldsymbol{\theta}^*, \mathbf{w}^*) &\leq \mathcal{L}_D(\boldsymbol{\theta}^*, \mathbf{w}) \text{ for all } \mathbf{w} \in \mathbb{R}^W, \\ \mathcal{L}_G(\boldsymbol{\theta}^*, \mathbf{w}^*) &\leq \mathcal{L}_G(\boldsymbol{\theta}, \mathbf{w}^*) \text{ for all } \boldsymbol{\theta} \in \mathbb{R}^\Theta \end{aligned}$$

satisfies (1). Hence, $(\boldsymbol{\theta}^*, \mathbf{w}^*) \in \mathbb{R}^\Theta \times \mathbb{R}^W$ satisfying (1) is called a *stationary local Nash equilibrium*.

2.2 Conjugate gradient methods

Let us consider a stationary point problem associated with unconstrained nonconvex optimization,

$$\text{find a point } \mathbf{x}^* \in \mathbb{R}^d \text{ such that } \nabla f(\mathbf{x}^*) = \mathbf{0}, \quad (2)$$

where $f: \mathbb{R}^d \rightarrow \mathbb{R}$ is continuously differentiable. There are many optimization methods [NW06, Chapters 3, 5, and 6] for solving problem (2), such as the steepest descent method, Newton method, quasi-Newton methods, and CG method. The CG method [NW06, Chapter 5], [HZ06] is defined as follows: given $\mathbf{x}_0 \in \mathbb{R}^d$ and $\mathbf{d}_0 := -\nabla f(\mathbf{x}_0)$,

$$\begin{aligned} \mathbf{x}_{n+1} &:= \mathbf{x}_n + \alpha_n \mathbf{d}_n, \\ \mathbf{d}_{n+1} &:= -\nabla f(\mathbf{x}_{n+1}) + \beta_{n+1} \mathbf{d}_n, \end{aligned} \quad (3)$$

where $(\alpha_n)_{n \in \mathbb{N}}$ is the sequence of step sizes (referred to as learning rates in the machine learning field), $\beta_{n+1} \in \mathbb{R}_+$, and \mathbf{d}_n denotes the search direction called the CG direction. The CG direction \mathbf{d}_{n+1} at time $n+1$ is computed from not only the current gradient $\nabla f(\mathbf{x}_{n+1})$ but also the past direction \mathbf{d}_n . Since algorithm (3) does not use any inverses of matrices, the method requires little memory. Overall, CG methods are divided into linear kind and the nonlinear kind.

The linear kind can solve a linear system of equations $A\mathbf{x} = \mathbf{b}$ with a positive definite matrix A and $\mathbf{b} \in \mathbb{R}^d$, which is equivalent to minimizing $f(\mathbf{x}) = (1/2)\langle \mathbf{x}, A\mathbf{x} \rangle - \langle \mathbf{b}, \mathbf{x} \rangle$ over \mathbb{R}^d . When the eigenvalues of A consist of m large values, with the $d - m$ smaller eigenvalues, a linear method will terminate at a solution after only $m + 1$ steps [NW06, Chapter 5.1].

The nonlinear kind has been widely studied (see also the following parameters β_n used in (3)) and has proved to be quite successful in practice [NW06, Chapter 5.2]. This implies that the nonlinear kind can be applied to a large-scale stationary point problem (2) with a general nonlinear function f .

Well-known parameters β_n for the nonlinear CG method (3) include the FR [FR64], PRP [PR69; Pol69], HS [HS52], and DY [DY99] formulas defined as follows:

$$\begin{aligned}\beta_n^{\text{FR}} &= \frac{\|\nabla f(\mathbf{x}_n)\|^2}{\|\nabla f(\mathbf{x}_{n-1})\|^2}, \quad \beta_n^{\text{PRP}} = \frac{\langle \nabla f(\mathbf{x}_n), \nabla f(\mathbf{x}_n) - \nabla f(\mathbf{x}_{n-1}) \rangle}{\|\nabla f(\mathbf{x}_{n-1})\|^2}, \\ \beta_n^{\text{HS}} &= \frac{\langle \nabla f(\mathbf{x}_n), \nabla f(\mathbf{x}_n) - \nabla f(\mathbf{x}_{n-1}) \rangle}{\langle \mathbf{d}_{n-1}, \nabla f(\mathbf{x}_n) - \nabla f(\mathbf{x}_{n-1}) \rangle}, \quad \beta_n^{\text{DY}} = \frac{\|\nabla f(\mathbf{x}_n)\|^2}{\langle \mathbf{d}_{n-1}, \nabla f(\mathbf{x}_n) - \nabla f(\mathbf{x}_{n-1}) \rangle}.\end{aligned}$$

The Hager–Zhang (HZ) [HZ05] formula is a modification of the HS formula; it is defined as follows:

$$\beta_n^{\text{HZ}} = \beta_n^{\text{HS}} - \mu \frac{\|\nabla f(\mathbf{x}_n) - \nabla f(\mathbf{x}_{n-1})\|^2 \langle \nabla f(\mathbf{x}_n), \mathbf{d}_{n-1} \rangle}{\langle \mathbf{d}_{n-1}, \nabla f(\mathbf{x}_n) - \nabla f(\mathbf{x}_{n-1}) \rangle^2},$$

where $\mu > 1/4$. The hybrid conjugate gradient method [DY01] combining the HS and DY methods uses

$$\beta_n = \max \{0, \min \{\beta_n^{\text{HS}}, \beta_n^{\text{DY}}\}\},$$

while the hybrid conjugate gradient method [HS91] combining the FR and PRP methods uses

$$\beta_n = \max \{0, \min \{\beta_n^{\text{FR}}, \beta_n^{\text{PRP}}\}\}.$$

The global convergence and convergence rate of the nonlinear CG methods with the above parameters β_n are described in [NW06, Chapter 5.2], [HS91], [DY01], and [HZ05].

2.3 Relationship and difference between conjugate gradient methods and momentum method

The momentum method (momentum SGD) [Pol64, (9)], [Sut+13, Section 2] is defined as follows: given $\mathbf{x}_0 \in \mathbb{R}^d$ and $\mathbf{m}_{-1} = \mathbf{0}$,

$$\begin{aligned}\mathbf{m}_n &:= -\epsilon \nabla f(\mathbf{x}_n) + \mu \mathbf{m}_{n-1}, \\ \mathbf{x}_{n+1} &:= \mathbf{x}_n + \mathbf{m}_n,\end{aligned}\tag{4}$$

where $\epsilon > 0$ is the learning rate and $\mu \in [0, 1]$ is the momentum coefficient. The momentum method (4) generates a sequence defined by

$$\mathbf{x}_{n+1} := \mathbf{x}_n - \epsilon \nabla f(\mathbf{x}_n) + \mu \mathbf{m}_{n-1},$$

while the CG method (3) generates a sequence defined by

$$\mathbf{x}_{n+1} := \mathbf{x}_n - \alpha_n \nabla f(\mathbf{x}_n) + \alpha_n \beta_n \mathbf{d}_{n-1},$$

where $\mathbf{d}_{-1} = \mathbf{0}$. Accordingly, the CG method (3) is a momentum method with a learning rate α_n and momentum coefficient $\alpha_n \beta_n$. While the momentum method (4) uses the momentum coefficient μ , the CG method (3) uses a momentum coefficient $\alpha_n \beta_n$ dependent of n through the CG parameters β_n listed in Subsection 2.2.

3 Conjugate Gradient Method for Local Nash Equilibrium Problem

The following algorithm for solving Problem 2.1 is based on the CG method. Algorithm 1 with $\beta_n^D = \beta_n^G = 0$ coincides with the SGD type of algorithm [Heu+17, (1)], i.e.,

$$\mathbf{w}_{n+1} = \mathbf{w}_n - b_n \mathcal{D}(\boldsymbol{\theta}_n, \mathbf{w}_n), \quad \boldsymbol{\theta}_{n+1} = \boldsymbol{\theta}_n - a_n \mathcal{G}(\boldsymbol{\theta}_n, \mathbf{w}_n).$$

See Sections 3.1.2 and 3.2.2 for examples of Algorithm 1.

Algorithm 1 Conjugate Gradient Method for Problem 2.1

Params: $(a_n)_{n \in \mathbb{N}}, (b_n)_{n \in \mathbb{N}} \subset \mathbb{R}_{++}, (\beta_n^D)_{n \in \mathbb{N}}, (\beta_n^G)_{n \in \mathbb{N}} \subset \mathbb{R}_+$
 1: $n \leftarrow 0, (\boldsymbol{\theta}_0, \mathbf{w}_0) \in \mathbb{R}^\Theta \times \mathbb{R}^W, \mathbf{d}^D(\boldsymbol{\theta}_{-1}, \mathbf{w}_{-1}) \in \mathbb{R}^\Theta, \mathbf{d}^G(\boldsymbol{\theta}_{-1}, \mathbf{w}_{-1}) \in \mathbb{R}^\Theta$
 2: **loop**
 3: $\mathbf{d}^D(\boldsymbol{\theta}_n, \mathbf{w}_n) := -\mathcal{D}(\boldsymbol{\theta}_n, \mathbf{w}_n) + \beta_n^D \mathbf{d}^D(\boldsymbol{\theta}_{n-1}, \mathbf{w}_{n-1})$
 4: $\mathbf{w}_{n+1} := \mathbf{w}_n + b_n \mathbf{d}^D(\boldsymbol{\theta}_n, \mathbf{w}_n)$
 5: $\mathbf{d}^G(\boldsymbol{\theta}_n, \mathbf{w}_n) := -\mathcal{G}(\boldsymbol{\theta}_n, \mathbf{w}_n) + \beta_n^G \mathbf{d}^G(\boldsymbol{\theta}_{n-1}, \mathbf{w}_{n-1})$
 6: $\boldsymbol{\theta}_{n+1} := \boldsymbol{\theta}_n + a_n \mathbf{d}^G(\boldsymbol{\theta}_n, \mathbf{w}_n)$
 7: $n \leftarrow n + 1$
 8: **end loop**

3.1 Constant learning rate rule

This subsection assumes the following:

Assumption 3.1

(C1) $a_n := a \in \mathbb{R}_{++}$ and $b_n := b \in \mathbb{R}_{++}$ for all $n \in \mathbb{N}$.

(C2) $\beta^D := \sup\{\beta_n^D : n \in \mathbb{N}\} \in [0, 1/2]$, $\beta^G := \sup\{\beta_n^G : n \in \mathbb{N}\} \in [0, 1/2]$.

(C3) The sequences of stochastic gradient errors $(M^{(\boldsymbol{\theta}_n)})_{n \in \mathbb{N}}$ and $(M^{(\mathbf{w}_n)})_{n \in \mathbb{N}}$ ensure that there exist $B_i \in \mathbb{R}_{++}$ ($i = 1, 2$) such that, for all $n \in \mathbb{N}$, $\mathbb{E}[\|M^{(\boldsymbol{\theta}_n)}\|^2] \leq B_1^2$ and $\mathbb{E}[\|M^{(\mathbf{w}_n)}\|^2] \leq B_2^2$.

(C4) $(\boldsymbol{\theta}_n)_{n \in \mathbb{N}}$ and $(\mathbf{w}_n)_{n \in \mathbb{N}}$ are almost surely bounded.²

Assumption (C2) is used to prove the boundedness of $(\mathbb{E}[\|\mathbf{d}^D(\boldsymbol{\theta}_n, \mathbf{w}_n)\|])_{n \in \mathbb{N}}$ and $(\mathbb{E}[\|\mathbf{d}^G(\boldsymbol{\theta}_n, \mathbf{w}_n)\|])_{n \in \mathbb{N}}$ (see Lemmas A.1 and A.2).³ If $(\mathbb{E}[\|\mathbf{d}^D(\boldsymbol{\theta}_n, \mathbf{w}_n)\|])_{n \in \mathbb{N}}$ and $(\mathbb{E}[\|\mathbf{d}^G(\boldsymbol{\theta}_n, \mathbf{w}_n)\|])_{n \in \mathbb{N}}$ are bounded, then (C2) can be omitted. Assumption (C3) is based on [Bor97, (1.7)] and [Heu+17, (A3)]. Assumption (C4) is the same as in [Heu+17, (A5)].

The following gives a convergence analysis as well as a convergence rate analysis of Algorithm 1 with constant learning rates. Section 3.1.2 illustrates some examples of Theorem 3.1.

Theorem 3.1 Suppose that Assumptions 2.1(A1)–(A2) and 3.1(C1)–(C4) hold and let B_i , C_i , and \tilde{K}_i ($i = 1, 2$) be positive constants independent of n (see Appendix for the definitions of the constants). Then, the following hold:

(i) [Convergence] For all $\boldsymbol{\theta} \in \mathbb{R}^\Theta$,

$$\liminf_{n \rightarrow +\infty} \mathbb{E}[\langle \boldsymbol{\theta}_n - \boldsymbol{\theta}, \nabla_{\boldsymbol{\theta}} \mathcal{L}_G(\boldsymbol{\theta}_n, \mathbf{w}_n) \rangle] \leq 2\tilde{K}_1^2 a + 2C_1\tilde{K}_1\beta^G + B_1C_1. \quad (5)$$

In particular, there exists a subsequence $((\boldsymbol{\theta}_{n_i}, \mathbf{w}_{n_i}))_{i \in \mathbb{N}}$ of $((\boldsymbol{\theta}_n, \mathbf{w}_n))_{n \in \mathbb{N}}$ such that $((\boldsymbol{\theta}_{n_i}, \mathbf{w}_{n_i}))_{i \in \mathbb{N}}$ converges almost surely to $(\boldsymbol{\theta}^*, \mathbf{w}^*)$ satisfying

$$\mathbb{E}[\|\nabla_{\boldsymbol{\theta}} \mathcal{L}_G(\boldsymbol{\theta}^*, \mathbf{w}^*)\|^2] \leq 2\tilde{K}_1^2 a + 2C_1\tilde{K}_1\beta^G + B_1C_1. \quad (6)$$

For all $\mathbf{w} \in \mathbb{R}^W$,

$$\liminf_{n \rightarrow +\infty} \mathbb{E}[\langle \mathbf{w}_n - \mathbf{w}, \nabla_{\mathbf{w}} \mathcal{L}_D(\boldsymbol{\theta}_n, \mathbf{w}_n) \rangle] \leq 2\tilde{K}_2^2 b + 2C_2\tilde{K}_2\beta^D + B_2C_2. \quad (7)$$

In particular, there exists a subsequence $((\boldsymbol{\theta}_{n_j}, \mathbf{w}_{n_j}))_{j \in \mathbb{N}}$ of $((\boldsymbol{\theta}_n, \mathbf{w}_n))_{n \in \mathbb{N}}$ such that $((\boldsymbol{\theta}_{n_j}, \mathbf{w}_{n_j}))_{j \in \mathbb{N}}$ converges almost surely to $(\boldsymbol{\theta}_*, \mathbf{w}_*)$ satisfying

$$\mathbb{E}[\|\nabla_{\mathbf{w}} \mathcal{L}_D(\boldsymbol{\theta}_*, \mathbf{w}_*)\|^2] \leq 2\tilde{K}_2^2 b + 2C_2\tilde{K}_2\beta^D + B_2C_2. \quad (8)$$

²The sequence $(\mathbf{x}_n)_{n \in \mathbb{N}} \subset \mathbb{R}^d$ is said to be almost surely bounded if $\sup\{\|\mathbf{x}_n\| : n \in \mathbb{N}\} < +\infty$ holds almost surely [Bor08, (2.1.4)].

³By referring to the proofs of Lemmas A.1 and A.2, we can check that (*) ensures the existence of $n_0 \in \mathbb{N}$ such that, for all $n \geq n_0$, $\beta_n^D, \beta_n^G \leq 1/2$ implies the boundedness of $(\mathbb{E}[\|\mathbf{d}^D(\boldsymbol{\theta}_n, \mathbf{w}_n)\|])_{n \in \mathbb{N}}$ and $(\mathbb{E}[\|\mathbf{d}^G(\boldsymbol{\theta}_n, \mathbf{w}_n)\|])_{n \in \mathbb{N}}$. This in turn implies that it is sufficient to assume the weaker condition (*) than (C2). In this paper, we use (C2) as a hypothesis for simplification.

(ii) [Convergence Rate] For all $\theta \in \mathbb{R}^\Theta$ and all $N \geq 1$,

$$\frac{1}{N} \sum_{n \in [N]} \mathbb{E} [\langle \theta_n - \theta, \nabla_\theta \mathcal{L}_G(\theta_n, \mathbf{w}_n) \rangle] \leq \frac{\mathbb{E}[\|\theta_1 - \theta\|^2]}{2aN} + 2\tilde{K}_1^2 a + 2C_1\tilde{K}_1\beta^G + B_1C_1. \quad (9)$$

For all $\mathbf{w} \in \mathbb{R}^W$ and all $N \geq 1$,

$$\frac{1}{N} \sum_{n \in [N]} \mathbb{E} [\langle \mathbf{w}_n - \mathbf{w}, \nabla_\mathbf{w} \mathcal{L}_D(\theta_n, \mathbf{w}_n) \rangle] \leq \frac{\mathbb{E}[\|\mathbf{w}_1 - \mathbf{w}\|^2]}{2bN} + 2\tilde{K}_2^2 b + 2C_2\tilde{K}_2\beta^D + B_2C_2. \quad (10)$$

If $((\theta_n, \mathbf{w}_n))_{n \in \mathbb{N}}$ converges almost surely to (θ^*, \mathbf{w}^*) ,⁴ then the convergent point (θ^*, \mathbf{w}^*) approximates a stationary local Nash equilibrium in the sense that

$$\begin{aligned} \mathbb{E} [\|\nabla_\theta \mathcal{L}_G(\theta^*, \mathbf{w}^*)\|^2] &\leq 2\tilde{K}_1^2 a + 2C_1\tilde{K}_1\beta^G + B_1C_1, \\ \mathbb{E} [\|\nabla_\mathbf{w} \mathcal{L}_D(\theta^*, \mathbf{w}^*)\|^2] &\leq 2\tilde{K}_2^2 b + 2C_2\tilde{K}_2\beta^D + B_2C_2 \end{aligned} \quad (11)$$

with convergence rates (9) and (10).

Properties (9), (10), and (11) in Theorem 3.1 indicate that, for sufficiently small learning rates a and b and CG parameters β^G and β^D ,

$$\mathbb{E} [\|\nabla_\theta \mathcal{L}_G(\theta^*, \mathbf{w}^*)\|^2] \approx 0, \quad \mathbb{E} [\|\nabla_\mathbf{w} \mathcal{L}_D(\theta^*, \mathbf{w}^*)\|^2] \approx 0$$

with

$$\frac{1}{N} \sum_{n \in [N]} \mathbb{E} [\langle \theta_n - \theta, \nabla_\theta \mathcal{L}_G(\theta_n, \mathbf{w}_n) \rangle] \approx \mathcal{O}\left(\frac{1}{N}\right), \quad \frac{1}{N} \sum_{n \in [N]} \mathbb{E} [\langle \mathbf{w}_n - \mathbf{w}, \nabla_\mathbf{w} \mathcal{L}_D(\theta_n, \mathbf{w}_n) \rangle] \approx \mathcal{O}\left(\frac{1}{N}\right), \quad (12)$$

where we assume that the stochastic gradient errors $M^{(\theta)}$ and $M^{(\mathbf{w})}$ are approximately zero.

3.1.1 Proof outline

Here, we provide a brief outline of the proof strategy of Theorem 3.1. The Appendix gives the detailed proof of Theorem 3.1. Assumptions 2.1(A1)–(A2) and 3.1(C2)–(C4) imply that $(\mathbb{E}[\|d^D(\theta_n, \mathbf{w}_n)\|])_{n \in \mathbb{N}}$ and $(\mathbb{E}[\|d^G(\theta_n, \mathbf{w}_n)\|])_{n \in \mathbb{N}}$ are bounded (Lemmas A.1 and A.2). Next, we evaluate the squared norm $\|\theta_{n+1} - \theta\|^2$ ($\theta \in \mathbb{R}^\Theta$) to find the relationship between $\|\theta_{n+1} - \theta\|$ and $\|\theta_n - \theta\|$. Using the expansion of the squared norm leads to that

$$\|\theta_{n+1} - \theta\|^2 \leq \|\theta_n - \theta\|^2 + 2a_n \langle \theta_n - \theta, d^G(\theta_n, \mathbf{w}_n) \rangle + a_n^2 \|d^G(\theta_n, \mathbf{w}_n)\|^2.$$

The definition of $d^G(\theta_n, \mathbf{w}_n)$ and the boundedness of $(\mathbb{E}[\|d^G(\theta_n, \mathbf{w}_n)\|])_{n \in \mathbb{N}}$ imply that there exist positive constants B_1 , C_1 , and \tilde{K}_1 , which depend on (A2), (C3), and (C4), such that, for all $n \in \mathbb{N}$,

$$\begin{aligned} \mathbb{E} [\|\theta_{n+1} - \theta\|^2] &\leq \mathbb{E} [\|\theta_n - \theta\|^2] + 2a_n \left(\mathbb{E} [\langle \theta - \theta_n, \nabla_\theta \mathcal{L}_G(\theta_n, \mathbf{w}_n) \rangle] + B_1C_1 + 2C_1\tilde{K}_1\beta_n^G \right) + 4\tilde{K}_1^2 a_n^2. \end{aligned} \quad (13)$$

Inequality (13) is a key inequality to prove Theorem 3.1. We can show (5) by contradiction and (13) with (C1). The limit inferior of $\mathbb{E}[\langle \theta_n - \theta, \nabla_\theta \mathcal{L}_G(\theta_n, \mathbf{w}_n) \rangle]$ in (5) ensures that there exists a subsequence $((\theta_{n_i}, \mathbf{w}_{n_i}))_{i \in \mathbb{N}}$ of $((\theta_n, \mathbf{w}_n))_{n \in \mathbb{N}}$ such that $((\theta_{n_i}, \mathbf{w}_{n_i}))_{i \in \mathbb{N}}$ converges almost surely to (θ^*, \mathbf{w}^*) satisfying that, for all $\theta \in \mathbb{R}^\Theta$,

$$\mathbb{E} [\langle \theta^* - \theta, \nabla_\theta \mathcal{L}_G(\theta^*, \mathbf{w}^*) \rangle] = \liminf_{n \rightarrow +\infty} \mathbb{E} [\langle \theta_n - \theta, \nabla_\theta \mathcal{L}_G(\theta_n, \mathbf{w}_n) \rangle],$$

which, together with $\theta := \theta^* - \nabla_\theta \mathcal{L}_G(\theta^*, \mathbf{w}^*)$, implies that

$$\mathbb{E} [\|\nabla_\theta \mathcal{L}_G(\theta^*, \mathbf{w}^*)\|^2] = \liminf_{n \rightarrow +\infty} \mathbb{E} [\langle \theta_n - (\theta^* - \nabla_\theta \mathcal{L}_G(\theta^*, \mathbf{w}^*)), \nabla_\theta \mathcal{L}_G(\theta_n, \mathbf{w}_n) \rangle].$$

Accordingly, we have (6). A discussion similar to the one for showing (13) leads to the following key inequality: there exist positive constants B_2 , C_2 , and \tilde{K}_2 , which depend on (A2), (C3), and (C4), such that, for all $n \in \mathbb{N}$,

$$\begin{aligned} \mathbb{E} [\|\mathbf{w}_{n+1} - \mathbf{w}\|^2] &\leq \mathbb{E} [\|\mathbf{w}_n - \mathbf{w}\|^2] + 2b_n \left(\mathbb{E} [\langle \mathbf{w} - \mathbf{w}_n, \nabla_\mathbf{w} \mathcal{L}_D(\theta_n, \mathbf{w}_n) \rangle] + B_2C_2 + 2C_2\tilde{K}_2\beta_n^D \right) + 4\tilde{K}_2^2 b_n^2. \end{aligned} \quad (14)$$

A discussion similar to the one for showing (5) and (6), together with (14), leads to (7) and (8). Summing (13) with (C1) from $n = 1$ to $n = N$ gives (9). Similarly, summing (14) from $n = 1$ to $n = N$ gives (10). Let us consider the case where $((\theta_n, \mathbf{w}_n))_{n \in \mathbb{N}}$ converges almost surely to (θ^*, \mathbf{w}^*) . Inequalities (6) and (8) thus guarantee (11).

⁴For example, the uniqueness of an accumulation point of $((\theta_n, \mathbf{w}_n))_{n \in \mathbb{N}}$ implies that this condition holds.

3.1.2 Examples of Algorithm 1 with constant learning rates

Let us discuss the results in Theorem 3.1 under certain conditions. For simplicity, we assume that $((\theta_n, w_n))_{n \in \mathbb{N}}$ generated by Algorithm 1 converges almost surely to (θ^*, w^*) and the stochastic gradient errors $M^{(\theta)}$ and $M^{(w)}$ are zero, i.e., $B_1 = B_2 = 0$.

(I) [SGD] First, we consider the case where $\beta^G = \beta^D = 0$. In this case, Algorithm 1 for the generator (resp. the discriminator) is based on the SGD method with a learning rate a (resp. b). Theorem 3.1 indicates that the convergent point of the SGD-type algorithm satisfies

$$\mathbb{E} \left[\|\nabla_{\theta} \mathcal{L}_G(\theta^*, w^*)\|^2 \right] \leq 2\tilde{K}_1^2 a, \quad \mathbb{E} \left[\|\nabla_w \mathcal{L}_D(\theta^*, w^*)\|^2 \right] \leq 2\tilde{K}_2^2 b.$$

(II) [Momentum SGD] We consider the case where $\beta_n^G := \beta^G \in [0, 1/2]$ and $\beta_n^D := \beta^D \in [0, 1/2]$. In this case, Algorithm 1 for the generator (resp. the discriminator) is based on the momentum method with a learning rate a (resp. b) and momentum coefficient $a\beta^G$ (resp. $b\beta^D$). Theorem 3.1 indicates that the convergent point of the momentum-type algorithm satisfies

$$\mathbb{E} \left[\|\nabla_{\theta} \mathcal{L}_G(\theta^*, w^*)\|^2 \right] \leq 2\tilde{K}_1^2 a + 2C_1\tilde{K}_1\beta^G, \quad \mathbb{E} \left[\|\nabla_w \mathcal{L}_D(\theta^*, w^*)\|^2 \right] \leq 2\tilde{K}_2^2 b + 2C_2\tilde{K}_2\beta^D. \quad (15)$$

(III) [CG] We consider the case where β_n^G and β_n^D are based on the CG formulas defined in Section 2.2. The parameters β_n^G and β_n^D satisfying (C2) are, for example, as follows:

$$\beta_n^G = \begin{cases} \beta_n^{\text{FR},G} = \begin{cases} \min \left\{ \frac{\|\mathcal{G}_n\|^2}{\|\mathcal{G}_{n-1}\|^2}, \frac{1}{2} \right\} & \text{if } \|\mathcal{G}_{n-1}\| \neq 0, \\ 0 & \text{otherwise} \end{cases} \\ \beta_n^{\text{PRP},G} = \begin{cases} \min \left\{ \frac{\langle \mathcal{G}_{n-1}, \mathcal{G}_n - \mathcal{G}_{n-1} \rangle}{\|\mathcal{G}_{n-1}\|^2}, \frac{1}{2} \right\} & \text{if } \|\mathcal{G}_{n-1}\| \neq 0, \\ 0 & \text{otherwise} \end{cases} \\ \beta_n^{\text{HS},G} = \begin{cases} \min \left\{ \frac{\langle \mathcal{G}_{n-1}, \mathcal{G}_n - \mathcal{G}_{n-1} \rangle}{\langle \mathcal{d}_{n-1}^G, \mathcal{G}_n - \mathcal{G}_{n-1} \rangle}, \frac{1}{2} \right\} & \text{if } \langle \mathcal{d}_{n-1}^G, \mathcal{G}_n - \mathcal{G}_{n-1} \rangle \neq 0, \\ 0 & \text{otherwise} \end{cases} \\ \beta_n^{\text{DY},G} = \begin{cases} \min \left\{ \frac{\|\mathcal{G}_n\|^2}{\langle \mathcal{d}_{n-1}^G, \mathcal{G}_n - \mathcal{G}_{n-1} \rangle}, \frac{1}{2} \right\} & \text{if } \langle \mathcal{d}_{n-1}^G, \mathcal{G}_n - \mathcal{G}_{n-1} \rangle \neq 0, \\ 0 & \text{otherwise} \end{cases} \\ \beta_n^{\text{HZ},G} = \begin{cases} \min \left\{ \beta_n^{\text{HS},G} - \mu \frac{\|\mathcal{G}_n - \mathcal{G}_{n-1}\|^2 \langle \mathcal{G}_n, \mathcal{d}_{n-1}^G \rangle}{\langle \mathcal{d}_{n-1}^G, \mathcal{G}_n - \mathcal{G}_{n-1} \rangle^2}, \frac{1}{2} \right\} & \text{if } \langle \mathcal{d}_{n-1}^G, \mathcal{G}_n - \mathcal{G}_{n-1} \rangle \neq 0, \\ 0 & \text{otherwise} \end{cases} \\ \beta_n^{\text{Hyb1},G} = \max \{0, \min \{\beta_n^{\text{HS},G}, \beta_n^{\text{DY},G}\}\} \\ \beta_n^{\text{Hyb2},G} = \max \{0, \min \{\beta_n^{\text{FR},G}, \beta_n^{\text{PRP},G}\}\} \end{cases} \quad (16)$$

where $\mathcal{G}_n := \mathcal{G}(\theta_n, w_n)$, $\mathcal{d}_n^G := \mathcal{d}^G(\theta_n, w_n)$, and $\mu > 1/4$.

$$\beta_n^D = \begin{cases} \beta_n^{\text{FR},D} = \begin{cases} \min \left\{ \frac{\|\mathcal{D}_n\|^2}{\|\mathcal{D}_{n-1}\|^2}, \frac{1}{2} \right\} & \text{if } \|\mathcal{D}_{n-1}\| \neq 0, \\ 0 & \text{otherwise} \end{cases} \\ \beta_n^{\text{PRP},D} = \begin{cases} \min \left\{ \frac{\langle \mathcal{D}_{n-1}, \mathcal{D}_n - \mathcal{D}_{n-1} \rangle}{\|\mathcal{D}_{n-1}\|^2}, \frac{1}{2} \right\} & \text{if } \|\mathcal{D}_{n-1}\| \neq 0, \\ 0 & \text{otherwise} \end{cases} \\ \beta_n^{\text{HS},D} = \begin{cases} \min \left\{ \frac{\langle \mathcal{D}_{n-1}, \mathcal{D}_n - \mathcal{D}_{n-1} \rangle}{\langle \mathcal{d}_{n-1}^D, \mathcal{D}_n - \mathcal{D}_{n-1} \rangle}, \frac{1}{2} \right\} & \text{if } \langle \mathcal{d}_{n-1}^D, \mathcal{D}_n - \mathcal{D}_{n-1} \rangle \neq 0, \\ 0 & \text{otherwise} \end{cases} \\ \beta_n^{\text{DY},D} = \begin{cases} \min \left\{ \frac{\|\mathcal{D}_n\|^2}{\langle \mathcal{d}_{n-1}^D, \mathcal{D}_n - \mathcal{D}_{n-1} \rangle}, \frac{1}{2} \right\} & \text{if } \langle \mathcal{d}_{n-1}^D, \mathcal{D}_n - \mathcal{D}_{n-1} \rangle \neq 0, \\ 0 & \text{otherwise} \end{cases} \\ \beta_n^{\text{HZ},D} = \begin{cases} \min \left\{ \beta_n^{\text{HS},D} - \mu \frac{\|\mathcal{D}_n - \mathcal{D}_{n-1}\|^2 \langle \mathcal{D}_n, \mathcal{d}_{n-1}^D \rangle}{\langle \mathcal{d}_{n-1}^D, \mathcal{D}_n - \mathcal{D}_{n-1} \rangle^2}, \frac{1}{2} \right\} & \text{if } \langle \mathcal{d}_{n-1}^D, \mathcal{D}_n - \mathcal{D}_{n-1} \rangle \neq 0, \\ 0 & \text{otherwise} \end{cases} \\ \beta_n^{\text{Hyb1},D} = \max \{0, \min \{\beta_n^{\text{HS},D}, \beta_n^{\text{DY},D}\}\} \\ \beta_n^{\text{Hyb2},D} = \max \{0, \min \{\beta_n^{\text{FR},D}, \beta_n^{\text{PRP},D}\}\} \end{cases} \quad (17)$$

where $\mathcal{D}_n := \mathcal{D}(\theta_n, w_n)$, $\mathcal{d}_n^D := \mathcal{d}^D(\theta_n, w_n)$, and $\mu > 1/4$. Theorem 3.1 indicates that the convergent point of the CG-type algorithm with β_n^G and β_n^D defined by (16) and (17) satisfies (15).

3.2 Diminishing learning rate rule

This subsection assumes the following:

Assumption 3.2

- (D1) For each $\theta \in \mathbb{R}^\Theta$, the ordinary differential equation $\dot{w}(t) = \nabla_w \mathcal{L}_D(\theta, w(t))$ has a local asymptotically stable attractor $\lambda(\theta)$ within a domain of attraction such that $\lambda: \mathbb{R}^\Theta \rightarrow \mathbb{R}^W$ is Lipschitz continuous. The ordinary differential equation $\dot{\theta}(t) = \nabla_\theta \mathcal{L}_G(\theta(t), \lambda(\theta(t)))$ has a local asymptotically stable attractor θ^* within a domain of attraction.
- (D2) $(a_n)_{n \in \mathbb{N}}$ and $(b_n)_{n \in \mathbb{N}}$ are monotone decreasing sequences satisfying either (i) or (ii):
 - (i) $\sum_{n=0}^{+\infty} a_n = +\infty$, $\sum_{n=0}^{+\infty} a_n^2 < +\infty$, $\sum_{n=0}^{+\infty} b_n = +\infty$, $\sum_{n=0}^{+\infty} b_n^2 < +\infty$, and $a_n = o(b_n)$;
 - (ii) $\lim_{n \rightarrow +\infty} (na_n)^{-1} = \lim_{n \rightarrow +\infty} (nb_n)^{-1} = 0$ and $\lim_{n \rightarrow +\infty} n^{-1} \sum_{k=0}^n a_k = \lim_{n \rightarrow +\infty} n^{-1} \sum_{k=0}^n b_k = 0$.
- (D3) The sequences of stochastic gradient errors $(M^{(\theta_n)})_{n \in \mathbb{N}}$ and $(M^{(w_n)})_{n \in \mathbb{N}}$ ensure that there exist $B_i \in \mathbb{R}_{++}$ ($i = 1, 2$) such that, for all $n \in \mathbb{N}$, $\|M^{(\theta_n)}\| \leq B_1$ and $\|M^{(w_n)}\| \leq B_2$ almost surely.
- (D4) $(\beta_n^D)_{n \in \mathbb{N}}$ and $(\beta_n^G)_{n \in \mathbb{N}}$ satisfy that $\lim_{n \rightarrow +\infty} n^{-1} \sum_{k=0}^n \beta_k^D = \lim_{n \rightarrow +\infty} n^{-1} \sum_{k=0}^n \beta_k^G = 0$.

Assumption (D1) is the same as in [Heu+17, (A4)] (see also [Bor97, (A1), (A2)]). Assumptions (D2)(i) [Heu+17, (A2)] and (D3) [Bor97, (1.7)] are needed to guarantee the almost-sure convergence of Algorithm 1, while Assumptions (D2)(ii) and (D4) are used to provide the rate of convergence of Algorithm 1.

The following presents a convergence analysis as well as a convergence rate analysis of Algorithm 1 with diminishing learning rates. Section 3.2.2 illustrates some examples of Theorem 3.2.

Theorem 3.2 Suppose that Assumptions 2.1(A1)–(A2) and 3.1(C2)–(C4) hold. Then, the following hold:

- (i) [Convergence] Under Assumption 3.2(D1), (D2)(i), and (D3), the sequence $((\theta_n, w_n))_{n \in \mathbb{N}}$ generated by Algorithm 1 converges almost surely to a point $(\theta^*, w^*) \in \text{LNE}(\mathcal{L}_D, \mathcal{L}_G)$.
- (ii) [Convergence Rate] Under Assumption 3.2(D2)(ii) and (D4),

$$\begin{aligned} \frac{1}{N} \sum_{n \in [N]} \mathbb{E} [\langle \theta_n - \theta, \nabla_\theta \mathcal{L}_G(\theta_n, w_n) \rangle] &\leq \frac{C_1^2}{2a_N N} + \frac{2C_1 \tilde{K}_1}{N} \sum_{n \in [N]} \beta_n^G + \frac{2\tilde{K}_1^2}{N} \sum_{n \in [N]} a_n + B_1 C_1, \\ \frac{1}{N} \sum_{n \in [N]} \mathbb{E} [\langle w_n - w, \nabla_w \mathcal{L}_D(\theta_n, w_n) \rangle] &\leq \frac{C_2^2}{2b_N N} + \frac{2C_2 \tilde{K}_2}{N} \sum_{n \in [N]} \beta_n^D + \frac{2\tilde{K}_2^2}{N} \sum_{n \in [N]} b_n + B_2 C_2. \end{aligned} \quad (18)$$

If we use $a_n = \mathcal{O}(n^{-\eta_a})$, $\beta_n^G = \mathcal{O}(n^{-\eta_a})$, $b_n = \mathcal{O}(n^{-\eta_b})$, and $\beta_n^D = \mathcal{O}(n^{-\eta_b})$, where $\eta_a, \eta_b \in (0, 1)$, then

$$\begin{aligned} \frac{1}{N} \sum_{n \in [N]} \mathbb{E} [\langle \theta_n - \theta, \nabla_\theta \mathcal{L}_G(\theta_n, w_n) \rangle] &\leq \mathcal{O}\left(\frac{1}{N^{\mu_a}}\right) + B_1 C_1, \\ \frac{1}{N} \sum_{n \in [N]} \mathbb{E} [\langle w_n - w, \nabla_w \mathcal{L}_D(\theta_n, w_n) \rangle] &\leq \mathcal{O}\left(\frac{1}{N^{\mu_b}}\right) + B_2 C_2, \end{aligned} \quad (19)$$

where $\mu_a := \min\{\eta_a, 1 - \eta_a\}$ and $\mu_b := \min\{\eta_b, 1 - \eta_b\}$.

Property (19) together with⁵

$$\eta_a = \eta_b = \frac{1}{2} \quad (20)$$

indicates that Algorithm 1 satisfies

$$\frac{1}{N} \sum_{n \in [N]} \mathbb{E} [\langle \theta_n - \theta, \nabla_\theta \mathcal{L}_G(\theta_n, w_n) \rangle] = \mathcal{O}\left(\frac{1}{\sqrt{N}}\right), \quad \frac{1}{N} \sum_{n \in [N]} \mathbb{E} [\langle w_n - w, \nabla_w \mathcal{L}_D(\theta_n, w_n) \rangle] = \mathcal{O}\left(\frac{1}{\sqrt{N}}\right), \quad (21)$$

⁵The maximum value of $\min\{\eta, 1 - \eta\}$ for $\eta \in (0, 1)$ is 1/2 when $\eta = 1/2$.

where we assume that the stochastic gradient errors $M^{(\theta)}$ and $M^{(w)}$ are zero. To guarantee that Algorithm 1 converges almost surely to a stationary Nash equilibrium, we need to set diminishing learning rates a_n and b_n satisfying Assumption 3.2(D2)(i), i.e.,

$$\frac{1}{2} < \eta_b < \eta_a < 1 \quad (22)$$

(see Theorem 3.2(i)). Then, property (19) ensures that Algorithm 1 has the following convergence rate:

$$\frac{1}{N} \sum_{n \in [N]} \mathbb{E} [\langle \boldsymbol{\theta}_n - \boldsymbol{\theta}, \nabla_{\boldsymbol{\theta}} \mathcal{L}_G(\boldsymbol{\theta}_n, \mathbf{w}_n) \rangle] = \mathcal{O}\left(\frac{1}{N^{\mu_a}}\right), \quad \frac{1}{N} \sum_{n \in [N]} \mathbb{E} [\langle \mathbf{w}_n - \mathbf{w}, \nabla_{\mathbf{w}} \mathcal{L}_D(\boldsymbol{\theta}_n, \mathbf{w}_n) \rangle] = \mathcal{O}\left(\frac{1}{N^{\mu_b}}\right), \quad (23)$$

where $\mu_a := \min\{\eta_a, 1 - \eta_a\}$ and $\mu_b := \min\{\eta_b, 1 - \eta_b\}$.

3.2.1 Proof outline

Here, we provide a brief outline of the proof strategy of Theorem 3.2. The Appendix gives the detailed proof of Theorem 3.2. The flow of the proof is the same as in [Bor97]. The definitions of $\boldsymbol{\theta}_{n+1}$ and \mathbf{w}_{n+1} imply that, for all $n \in \mathbb{N}$,

$$\begin{aligned} \boldsymbol{\theta}_{n+1} &= \boldsymbol{\theta}_n - b_n \frac{a_n}{b_n} \mathcal{G}(\boldsymbol{\theta}_n, \mathbf{w}_n) + a_n \beta_n^G \mathbf{d}^G(\boldsymbol{\theta}_{n-1}, \mathbf{w}_{n-1}), \\ \mathbf{w}_{n+1} &= \mathbf{w}_n - b_n \mathcal{D}(\boldsymbol{\theta}_n, \mathbf{w}_n) + b_n \beta_n^D \mathbf{d}^D(\boldsymbol{\theta}_{n-1}, \mathbf{w}_{n-1}). \end{aligned} \quad (24)$$

We can check that (24) is regarded as a discretized version of the ordinary differential equations $\dot{\mathbf{x}}(t) = \mathbf{0}$ and $\dot{\mathbf{y}}(t) = \mathcal{D}(\mathbf{x}(t), \mathbf{y}(t))$ with a step size b_n and errors at the n th iteration defined by

$$-\frac{a_n}{b_n} \mathcal{G}(\boldsymbol{\theta}_n, \mathbf{w}_n) + a_n \beta_n^G \mathbf{d}^G(\boldsymbol{\theta}_{n-1}, \mathbf{w}_{n-1}) \text{ and } b_n \beta_n^D \mathbf{d}^D(\boldsymbol{\theta}_{n-1}, \mathbf{w}_{n-1}). \quad (25)$$

Assumptions 3.1(C2), 3.2(D2)(i), and (D3) thus guarantee that two sequences defined by (25) converge almost surely to zero. Hence, an argument similar to the one for obtaining Theorem 1.1 in [Bor97] (see [Bor97, Section 2] for the detailed proof) leads to Theorem 3.2(i). Theorem 3.2(ii) depends on the key inequalities (13) and (14), which come from Assumptions 2.1(A1)–(A2) and 3.1(C2)–(C4). Summing (13) and (14) from $n = 1$ to $n = N$ gives (18). In particular, let us define $a_n = \mathcal{O}(n^{-\eta_a})$, $\beta_n^G = \mathcal{O}(n^{-\eta_a})$, $b_n = \mathcal{O}(n^{-\eta_b})$, and $\beta_n^D = \mathcal{O}(n^{-\eta_b})$, where $\eta_a, \eta_b \in (0, 1)$. These learning rates satisfy Assumption 3.2(D2)(ii) and (D4). Hence, (18) implies (19).

3.2.2 Examples of Algorithm 1 with diminishing learning rates

Let us discuss the results in Theorem 3.2 under certain conditions. For simplicity, we assume that the stochastic gradient errors $M^{(\theta)}$ and $M^{(w)}$ are zero, i.e., $B_1 = B_2 = 0$.

(I) [SGD] First, we consider the case where $\beta^G = \beta^D = 0$. In this case, Algorithm 1 for the generator (resp. the discriminator) is based on the SGD method with a learning rate a_n (resp. b_n). This algorithm was presented in [Heu+17, (1)]. Theorem 3.2(ii) indicates that the SGD-type algorithm satisfies (21) and (23); i.e.,

$$\begin{aligned} \frac{1}{N} \sum_{n \in [N]} \mathbb{E} [\langle \boldsymbol{\theta}_n - \boldsymbol{\theta}, \nabla_{\boldsymbol{\theta}} \mathcal{L}_G(\boldsymbol{\theta}_n, \mathbf{w}_n) \rangle] &= \begin{cases} \mathcal{O}\left(\frac{1}{\sqrt{N}}\right) & \text{if (20) holds,} \\ \mathcal{O}\left(\frac{1}{N^{\mu_a}}\right) & \text{if (22) holds,} \end{cases} \\ \frac{1}{N} \sum_{n \in [N]} \mathbb{E} [\langle \mathbf{w}_n - \mathbf{w}, \nabla_{\mathbf{w}} \mathcal{L}_D(\boldsymbol{\theta}_n, \mathbf{w}_n) \rangle] &= \begin{cases} \mathcal{O}\left(\frac{1}{\sqrt{N}}\right) & \text{if (20) holds,} \\ \mathcal{O}\left(\frac{1}{N^{\mu_b}}\right) & \text{if (22) holds.} \end{cases} \end{aligned}$$

(II) [Momentum SGD] Let us consider Algorithm 1 for the generator (resp. the discriminator) based on the momentum method with a learning rate a_n (resp. b_n) and momentum coefficient $a_n \beta_n^G$ (resp. $b_n \beta_n^D$). Let us consider β_n^G and β_n^D with (22). Then, there exists $n_1 \in \mathbb{N}$ such that, for all $n \geq n_1$, $\beta_n^G, \beta_n^D \leq 1/2$, which implies that β_n^G and β_n^D satisfy (C2). Theorem 3.2(ii) thus ensures that the momentum-type algorithm has the same convergence rate as in (I).

(III) [CG] Let us consider the CG-type algorithm, i.e., Algorithm 1 with a_n and b_n with (20) and β_n^G and β_n^D defined by (16) and (17). Theorem 3.2(i) guarantees that the CG-type algorithm converges almost surely to a point in

LNE($\mathcal{L}_D, \mathcal{L}_G$). Next, let us consider β_n^G and β_n^D defined as follows:

$$\beta_n^G = \begin{cases} \beta_n^{\text{FR},G} = \begin{cases} \min \left\{ \frac{\|\mathcal{G}_n\|^2}{\|\mathcal{G}_{n-1}\|^2}, \frac{1}{2} \right\} \frac{1}{n^{\eta_a}} & \text{if } \|\mathcal{G}_{n-1}\| \neq 0, \\ 0 & \text{otherwise} \end{cases} \\ \beta_n^{\text{PRP},G} = \begin{cases} \min \left\{ \frac{\langle \mathcal{G}_{n-1}, \mathcal{G}_n - \mathcal{G}_{n-1} \rangle}{\|\mathcal{G}_{n-1}\|^2}, \frac{1}{2} \right\} \frac{1}{n^{\eta_a}} & \text{if } \|\mathcal{G}_{n-1}\| \neq 0, \\ 0 & \text{otherwise} \end{cases} \\ \beta_n^{\text{HS},G} = \begin{cases} \min \left\{ \frac{\langle \mathcal{G}_{n-1}, \mathcal{G}_n - \mathcal{G}_{n-1} \rangle}{\langle \mathcal{d}_{n-1}^G, \mathcal{G}_n - \mathcal{G}_{n-1} \rangle}, \frac{1}{2} \right\} \frac{1}{n^{\eta_a}} & \text{if } \langle \mathcal{d}_{n-1}^G, \mathcal{G}_n - \mathcal{G}_{n-1} \rangle \neq 0, \\ 0 & \text{otherwise} \end{cases} \\ \beta_n^{\text{DY},G} = \begin{cases} \min \left\{ \frac{\|\mathcal{G}_n\|^2}{\langle \mathcal{d}_{n-1}^G, \mathcal{G}_n - \mathcal{G}_{n-1} \rangle}, \frac{1}{2} \right\} \frac{1}{n^{\eta_a}} & \text{if } \langle \mathcal{d}_{n-1}^G, \mathcal{G}_n - \mathcal{G}_{n-1} \rangle \neq 0, \\ 0 & \text{otherwise} \end{cases} \\ \beta_n^{\text{HZ},G} = \begin{cases} \min \left\{ \beta_n^{\text{HS},G} - \mu \frac{\|\mathcal{G}_n - \mathcal{G}_{n-1}\|^2 \langle \mathcal{G}_n, \mathcal{d}_{n-1}^G \rangle}{\langle \mathcal{d}_{n-1}^G, \mathcal{G}_n - \mathcal{G}_{n-1} \rangle^2}, \frac{1}{2} \right\} \frac{1}{n^{\eta_a}} & \text{if } \langle \mathcal{d}_{n-1}^G, \mathcal{G}_n - \mathcal{G}_{n-1} \rangle \neq 0, \\ 0 & \text{otherwise} \end{cases} \\ \beta_n^{\text{Hyb1},G} = \max \left\{ 0, \min \left\{ \beta_n^{\text{HS},G}, \beta_n^{\text{DY},G} \right\} \right\} \\ \beta_n^{\text{Hyb2},G} = \max \left\{ 0, \min \left\{ \beta_n^{\text{FR},G}, \beta_n^{\text{PRP},G} \right\} \right\} \end{cases} \quad (26)$$

where $\mathcal{G}_n := \mathcal{G}(\boldsymbol{\theta}_n, \mathbf{w}_n)$, $\mathcal{d}_n^G := \mathcal{d}^G(\boldsymbol{\theta}_n, \mathbf{w}_n)$, and $\mu > 1/4$.

$$\beta_n^D = \begin{cases} \beta_n^{\text{FR},D} = \begin{cases} \min \left\{ \frac{\|\mathcal{D}_n\|^2}{\|\mathcal{D}_{n-1}\|^2}, \frac{1}{2} \right\} \frac{1}{n^{\eta_b}} & \text{if } \|\mathcal{D}_{n-1}\| \neq 0, \\ 0 & \text{otherwise} \end{cases} \\ \beta_n^{\text{PRP},D} = \begin{cases} \min \left\{ \frac{\langle \mathcal{D}_{n-1}, \mathcal{D}_n - \mathcal{D}_{n-1} \rangle}{\|\mathcal{D}_{n-1}\|^2}, \frac{1}{2} \right\} \frac{1}{n^{\eta_b}} & \text{if } \|\mathcal{D}_{n-1}\| \neq 0, \\ 0 & \text{otherwise} \end{cases} \\ \beta_n^{\text{HS},D} = \begin{cases} \min \left\{ \frac{\langle \mathcal{D}_{n-1}, \mathcal{D}_n - \mathcal{D}_{n-1} \rangle}{\langle \mathcal{d}_{n-1}^D, \mathcal{D}_n - \mathcal{D}_{n-1} \rangle}, \frac{1}{2} \right\} \frac{1}{n^{\eta_b}} & \text{if } \langle \mathcal{d}_{n-1}^D, \mathcal{D}_n - \mathcal{D}_{n-1} \rangle \neq 0, \\ 0 & \text{otherwise} \end{cases} \\ \beta_n^{\text{DY},D} = \begin{cases} \min \left\{ \frac{\|\mathcal{D}_n\|^2}{\langle \mathcal{d}_{n-1}^D, \mathcal{D}_n - \mathcal{D}_{n-1} \rangle}, \frac{1}{2} \right\} \frac{1}{n^{\eta_b}} & \text{if } \langle \mathcal{d}_{n-1}^D, \mathcal{D}_n - \mathcal{D}_{n-1} \rangle \neq 0, \\ 0 & \text{otherwise} \end{cases} \\ \beta_n^{\text{HZ},D} = \begin{cases} \min \left\{ \beta_n^{\text{HS},D} - \mu \frac{\|\mathcal{D}_n - \mathcal{D}_{n-1}\|^2 \langle \mathcal{D}_n, \mathcal{d}_{n-1}^D \rangle}{\langle \mathcal{d}_{n-1}^D, \mathcal{D}_n - \mathcal{D}_{n-1} \rangle^2}, \frac{1}{2} \right\} \frac{1}{n^{\eta_b}} & \text{if } \langle \mathcal{d}_{n-1}^D, \mathcal{D}_n - \mathcal{D}_{n-1} \rangle \neq 0, \\ 0 & \text{otherwise} \end{cases} \\ \beta_n^{\text{Hyb1},D} = \max \left\{ 0, \min \left\{ \beta_n^{\text{HS},D}, \beta_n^{\text{DY},D} \right\} \right\} \\ \beta_n^{\text{Hyb2},D} = \max \left\{ 0, \min \left\{ \beta_n^{\text{FR},D}, \beta_n^{\text{PRP},D} \right\} \right\} \end{cases} \quad (27)$$

where $\mathcal{D}_n := \mathcal{D}(\boldsymbol{\theta}_n, \mathbf{w}_n)$, $\mathcal{d}_n^D := \mathcal{d}^D(\boldsymbol{\theta}_n, \mathbf{w}_n)$, and $\mu > 1/4$. The sequences $(\beta_n^G)_{n \in \mathbb{N}}$ and $(\beta_n^D)_{n \in \mathbb{N}}$ defined by (26) and (27) satisfy (C2) and (D4). Property (19) ensures that the CG-type algorithm has the same convergence rate as in (I).

4 Numerical Experiments

4.1 Overview

This experimental section consists of two parts. The first examines the convergence of SGD, momentum SGD, and CG methods to a local Nash equilibrium when they use constant and diminishing learning rate scheduling in minimax optimization. In the second part, since we apply CG methods to the GANs problem setting as a first attempt, we compare and evaluate the CG method against SGD and momentum SGD. In particular, we start by showing the trajectories of these methods on two learning rate schedules in a toy problem setting. Then, we extend the experimental setting to training on real-world datasets (MNIST and CIFAR10).

4.2 Toy example

As an objective function, we chose $f(x, y) = (1 + x^2) \cdot (100 - y^2)$. The problem setting was one in which x is minimized with the derivative $f_x = 2x \cdot (100 - y^2)$ as the gradient direction and y is maximized with the derivative $f_y = -2y \cdot (1 + x^2)$ as the gradient direction. With the objective function under $f(x, y) = (1 + x^2) \cdot (100 - y^2)$, the local Nash equilibrium is $(x, y) = (0, 0)$.

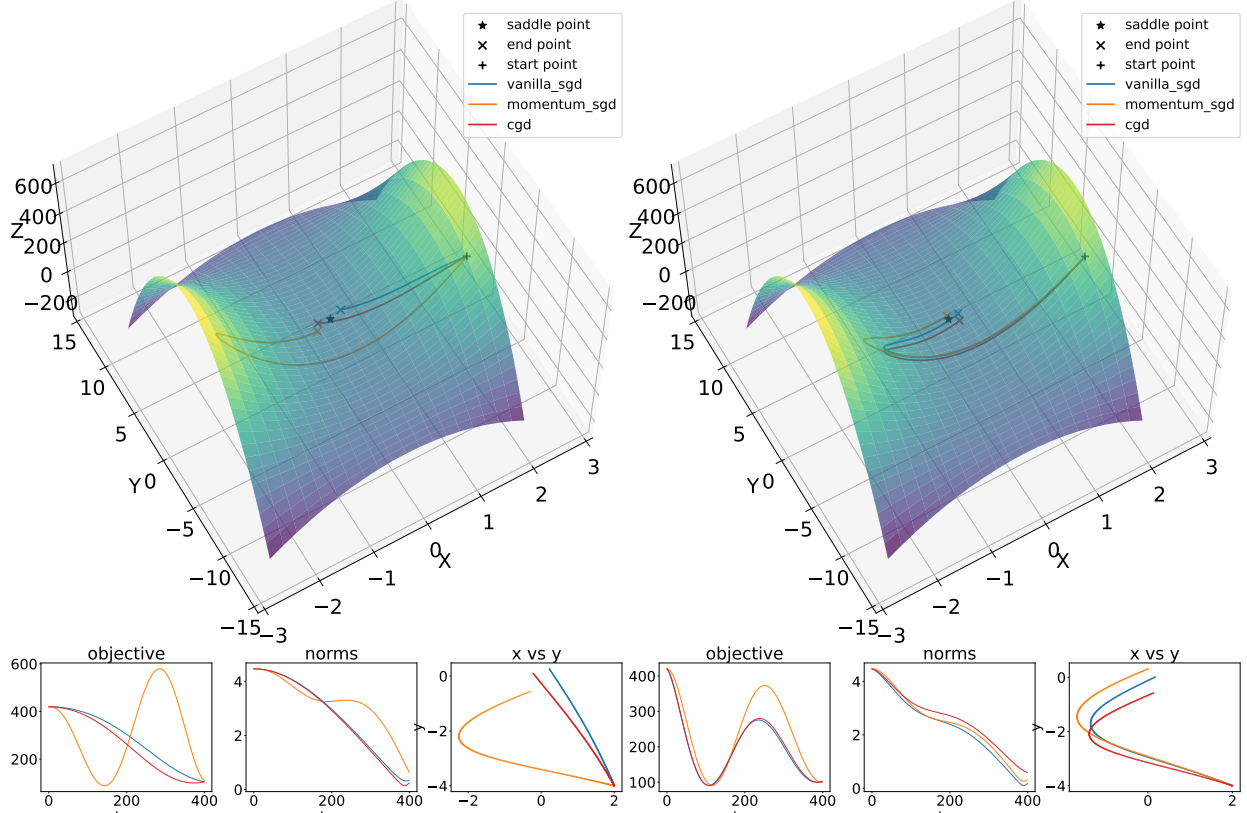


Figure 2. Toy example of minimax optimization using SGD, momentum SGD, and CG methods. Objective function: $f(x, y) = (1 + x^2) \cdot (100 - y^2)$. **Top Left:** trajectory of optimization with constant learning rate schedule, **Top Right:** trajectory of optimization with inverse square learning rate schedule, **Bottom Left:** objective, norms, and x vs. y with constant learning rate schedule, **Bottom Right:** objective, norms, and x vs. y with inverse square learning rate schedule. We tuned the initial learning rate for each optimization method. Details are given in Appendix C.3.

The trajectory of optimization is shown in Figure 2 for either a constant learning rate or diminishing learning rate with $\eta_a = \eta_b = 0.5$. This toy example confirms convergence to a local Nash equilibrium for an appropriate learning rate. We can see that each optimizer follows a different trajectory, but eventually reaches the same convergence point. The objective oscillates, but converges $f(x, y) = 100$ (the value of the objective at the local Nash equilibrium), and the norm decreases almost monotonically.

4.3 Real-world data experiments

We conducted a series of experiments using DCGAN [RMC15], which is used in the PyTorch official example⁶. In order to follow Assumptions 2.1(A2), we replaced the BN layer with a spectral normalization layer [Miy+18].

In this experimental setting, the loss function is high-dimensional and non-convex, so a simple gradient norm does not necessarily correspond to the quality of learning of the GANs. Here, the Fréchet inception distance (FID) [Heu+17] is commonly used to evaluate the quality of learning of GANs, so we chose it as a metric to evaluate the training on real-world data. FID is measured on the basis of statistical information obtained by transforming real and fake images using a neural network. The smaller the value of this metric is, the better the training of the generator of the GANs becomes.

Comparing the FID scores of the trained model by the CG method and the other optimizers in Table 3 reveals that the CG methods outperformed the conventional optimizers (SGD and momentum SGD) in the case of the constant learning rate schedule. We tested the seven beta update rules described in Section 2.2. For the hyperparameter search, we conducted a grid search for all optimizers and datasets. The details of the hyperparameters are in Appendix C.3, and the remaining experimental settings are detailed in Appendix C.

⁶https://pytorch.org/tutorials/beginner/dcgan_faces_tutorial.html

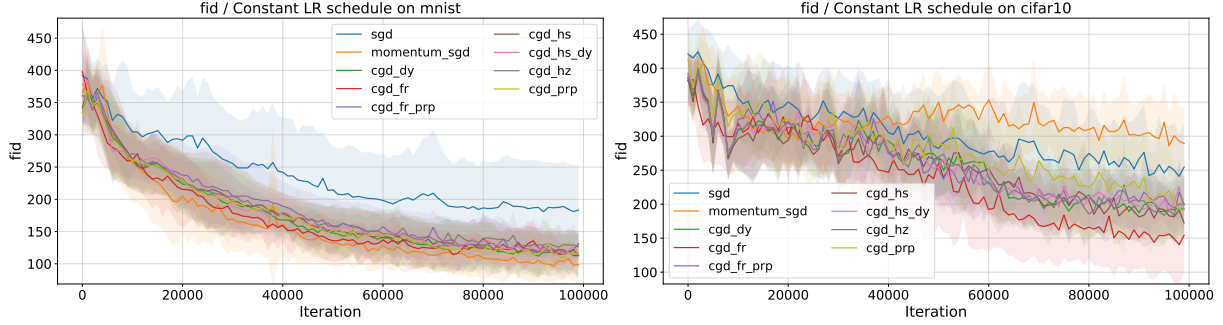


Figure 3. Mean FID (solid line) bounded by the maximum and minimum over best 10 runs (the shaded areas) in sense of FID. **Left:** MNIST and constant learning rate, **Right:** CIFAR-10 and constant learning rate

Dataset	LR Schedule	sgd	momentum_sgd	cgd_dy	cgd_fr	cgd_fr_prp	cgd_hs	cgd_hs_dy	cgd_hz	cgd_prp
MNIST	Constant	67.96	50.74	40.29	84.60	52.27	99.25	64.14	83.10	46.88
CIFAR10	Constant	133.73	194.12	115.38	82.29	140.96	142.97	140.05	148.33	121.41
MNIST	Diminishing	314.90	143.95	314.79	295.19	308.22	308.22	308.22	309.78	308.22
CIFAR10	Diminishing	339.69	225.72	330.11	288.99	334.84	323.80	334.84	362.92	345.54

Table 3: Best FID scores for two datasets and two learning rate schedules. **Best scores** are in **bold** and **second best scores** are in **blue** for constant learning rate scheduling. The FID scores in the diminishing learning rate experiment, in **gray**, were significantly degraded for all optimizers.

4.3.1 Constant learning rate schedule

To the best of our knowledge, a constant learning rate is practically used for training GANs, including those in [Heu+17]. Before conducting the diminishing learning rate experiment, we compared the training behaviors of the CG method, SGD, and momentum SGD when using a constant learning rate schedule. In addition to the FID score (Figure 3), we calculated the loss (Figure 6 in Appendix D.1) and the gradient norm of each generator and discriminator (Figure 7 in Appendix D.1).

Table 3 shows the best (lowest) FID of each optimizer for training on the MNIST and CIFAR10 datasets. In the MNIST case, the CG method (DY β update rule) achieved a lower FID score than SGD and momentum SGD. In the CIFAR10 case, the CG method (FR β update rule) achieved a lower FID score than SGD and momentum SGD especially in the constant learning rate setting.

In the MNIST case, the discriminator’s loss decreased steadily, increasing the generator’s loss. The CG method using DY as a β update rule had the best FID score: the discriminator’s loss decreased steadily, and the generator’s loss increased, suggesting convergence to the saddle point. In the case of CIFAR10, the generator’s loss oscillated significantly in the early stage of learning, and the discriminator’s loss decreased accordingly. We found that the loss did not necessarily converge to 0.

Finally, Tables 4 and 5 show that the norms of gradients in the constant learning rate case are close to 0, suggesting that the training with the best hyperparameter in the sense of FID converges to a local Nash equilibrium.

4.3.2 Diminishing learning rate schedule

The inverse square learning rate was not used in the previous studies [Heu+17; Goo17; RMC15] because of the rapid decay of the learning rate from the beginning to the middle of the learning process, which is challenging to balance in minimax optimization. The results of those studies show that the FID scores tend to remain high compared to those for the constant learning rate for all optimizers and the two datasets.

The third and forth row of Tables 3, 4, and 5 show the gradient norm and the best (lowest) FID for all optimizers. Not only was FID significantly worse than in the case of the constant learning rate schedule, but also the gradient norm was much higher.

The losses of each generator and discriminator for training on the MNIST and CIFAR10 are shown in Appendix D.2. The details of the FID scores for each learning-rate combination of are shown in Figures 12 and 13 in Appendix E.1.

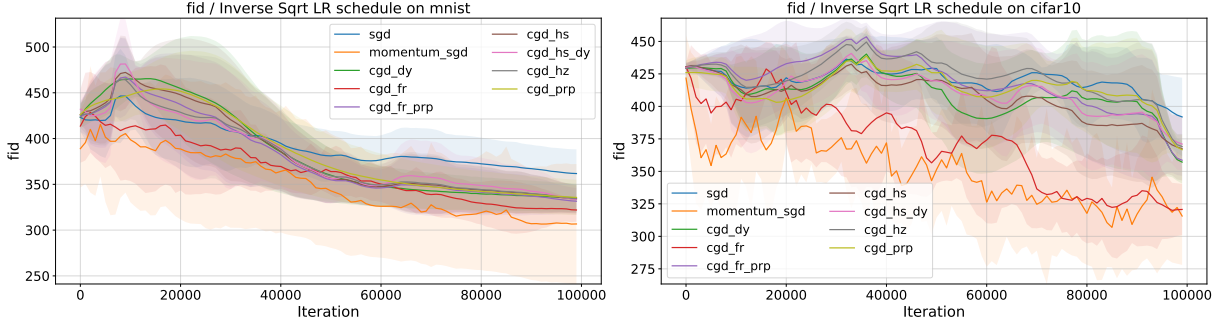


Figure 4. Mean FID (solid line) bounded by the maximum and minimum (the shaded areas) over best 10 percentile runs in sense of FID. **Left:** Results for MNIST and inverse sqrt learning rate, **Right:** Results for CIFAR-10 and inverse sqrt learning rate.

Regarding training with the diminishing learning rate, the schedule with the largest learning rate tended to give the best FID score; since the learning rate with the diminishing learning rate schedule ϵ smaller than that of the constant learning rate schedule, it may be necessary to expand the search range of the learning rate, but this might cause instability in the early stages of training. For all optimizers, the learning with the diminishing learning rate schedule always underperformed the learning with the constant learning rate schedule.

5 Conclusion

For training GANs, we proposed CG-type algorithms to solve local Nash equilibrium problems and proved their convergence to local Nash equilibria under constant and diminishing learning rates under mild assumptions; furthermore, we analyzed the convergence rates of the SGD, momentum SGD, and CG methods. We compared our method with SGD and momentum SGD on a toy problem that gave experimental results consistent with theory. Finally, we evaluated the optimizer by training GANs using the FID score as a metric and showed that under constant learning rates, the CG method outperformed SGD and momentum SGD in two real-world problem settings.

One limitation of this study is that it involved experiments on only two datasets. Although the CG method minimized the FID scores in both cases, validations on other real-world datasets will be needed in order to support our claims. Another limitation is the unsuccessful training with the diminishing learning rate in practice. The diminishing learning rate has been used in previous studies to provide theoretical proof of convergence to local Nash equilibria, but not in practical experiments. We have given a proof for a constant learning rate and obtained results that suggest that the diminishing learning rate does not work in experiments even with an extensive hyperparameter search. Although we

Dataset	LR Schedule	sgd	momentum_sgd	cgd_dy	cgd_fr	cgd_fr_prp	cgd_hs	cgd_hs_dy	cgd_hz	cgd_prp
MINIST	Constant	3.1e-02	0.0e+00	3.0e-02	2.7e-02	3.4e-02	3.3e-02	3.4e-02	3.5e-02	3.4e-02
CIFAR10	Constant	6.4e-04	0.0e+00	1.8e-02	9.3e-04	2.0e-02	1.5e-02	2.5e-02	2.0e-02	1.5e-02
MINIST	Diminishing	6.0e-02	3.0e-02	6.0e-02	4.9e-02	6.0e-02	6.0e-02	6.0e-02	6.0e-02	6.0e-02
CIFAR10	Diminishing	9.7e-02	6.4e-02	9.6e-02	8.5e-02	9.6e-02	9.6e-02	9.6e-02	9.6e-02	8.5e-02

Table 4: Norm of generator’s gradients where FID score is the best for two datasets and two learning rate schedules. **Best scores** in the sense of FID are in **bold** and **second best scores** are in **blue** for constant learning rate scheduling. The FID scores in the diminishing learning rate experiment, in **gray**, were significantly degraded for all optimizers.

Dataset	LR Schedule	sgd	momentum_sgd	cgd_dy	cgd_fr	cgd_fr_prp	cgd_hs	cgd_hs_dy	cgd_hz	cgd_prp
MINIST	Constant	7.2e-05	1.8e-09	1.3e-04	1.6e-05	6.4e-05	7.5e-05	1.4e-04	8.1e-05	6.7e-05
CIFAR10	Constant	1.5e-04	1.1e-05	2.3e-04	8.4e-05	1.1e-04	1.0e-04	1.7e-04	2.5e-04	1.3e-04
MINIST	Diminishing	4.0e-01	3.8e-02	4.0e-01	2.8e-01	3.2e-01	4.0e-01	4.0e-01	4.0e-01	4.0e-01
CIFAR10	Diminishing	1.9e-01	1.3e-01	2.2e-01	2.2e-01	1.7e-01	2.2e-01	2.2e-01	2.2e-01	2.2e-01

Table 5: Norm of discriminator’s gradients where FID score is the best for two datasets and two learning rate schedules. **Best scores** in the sense of FID are in **bold** and **second best scores** are in **blue** for constant learning rate scheduling. The FID scores in the diminishing learning rate experiment, in **gray**, were significantly degraded for all optimizers.

have proven convergence to a local Nash equilibrium with a diminishing learning rate, there is a gap between theory and practice, and research is needed to bridge this gap.

Acknowledgments

We would like to thank Tetsuya Motokawa (Retty Inc.) for his help on the PyTorch implementation. This work was supported by the Masason Foundation Fellowship awarded to Hiroki Naganuma and by the Japan Society for the Promotion of Science (JSPS) KAKENHI Grant Number 21K11773 awarded to Hideaki Iiduka. The computation resource of this project is supported by ABCI⁷.

References

- [Nas51] John Nash. “Non-Cooperative Games”. In: *Annals of Mathematics* 54.2 (1951), pp. 286–295. ISSN: 0003486X. URL: <http://www.jstor.org/stable/1969529>.
- [HS52] M. Hestenes and E. Stiefel. “Methods of conjugate gradients for solving linear systems”. In: *Journal of research of the National Bureau of Standards* 49 (1952), pp. 409–435.
- [FR64] R. Fletcher and C. M. Reeves. “Function minimization by conjugate gradients”. In: *The Computer Journal* 7.2 (1964), pp. 149–154.
- [Pol64] B. T. Polyak. “Some methods of speeding up the convergence of iteration methods”. In: *USSR Computational Mathematics and Mathematical Physics* 4 (1964), pp. 1–17.
- [PR69] E. Polak and G. Ribiere. “Note sur la convergence de méthodes de directions conjuguées”. fr. In: *ESAIM: Mathematical Modelling and Numerical Analysis - Modélisation Mathématique et Analyse Numérique* 3.R1 (1969), pp. 35–43. URL: http://www.numdam.org/item/M2AN_1969__3_1_35_0/.
- [Pol69] B.T. Polyak. “The conjugate gradient method in extremal problems”. In: *USSR Computational Mathematics and Mathematical Physics* 9.4 (1969), pp. 94–112. ISSN: 0041-5553. DOI: [https://doi.org/10.1016/0041-5553\(69\)90035-4](https://doi.org/10.1016/0041-5553(69)90035-4). URL: <https://www.sciencedirect.com/science/article/pii/0041555369900354>.
- [HS91] Y. Hu and C. Storey. “Global convergence result for conjugate gradient methods”. In: *Journal of Optimization Theory and Applications* 72 (1991), pp. 399–405.
- [Møl93] Martin Fodslette Møller. “A scaled conjugate gradient algorithm for fast supervised learning”. In: *Neural Networks* 6.4 (1993), pp. 525–533. ISSN: 0893-6080. DOI: [https://doi.org/10.1016/S0893-6080\(05\)80056-5](https://doi.org/10.1016/S0893-6080(05)80056-5). URL: <https://www.sciencedirect.com/science/article/pii/S0893608005800565>.
- [Bor97] Vivek S. Borkar. “Stochastic approximation with two time scales”. In: *Systems & Control Letters* 29.5 (1997), pp. 291–294. ISSN: 0167-6911. DOI: [https://doi.org/10.1016/S0167-6911\(97\)90015-3](https://doi.org/10.1016/S0167-6911(97)90015-3). URL: <https://www.sciencedirect.com/science/article/pii/S0167691197900153>.
- [DY99] Y. H. Dai and Y. Yuan. “A Nonlinear Conjugate Gradient Method with a Strong Global Convergence Property”. In: *SIAM Journal on Optimization* 10.1 (1999), pp. 177–182. DOI: [10.1137/S1052623497318992](https://doi.org/10.1137/S1052623497318992). eprint: <https://doi.org/10.1137/S1052623497318992>. URL: <https://doi.org/10.1137/S1052623497318992>.
- [DY01] Y. H. Dai and Y. Yuan. “An Efficient Hybrid Conjugate Gradient Method for Unconstrained Optimization”. In: *Annals of Operations Research* 103 (2001), pp. 33–47.
- [HZ05] W. W. Hager and H. Zhang. “A New Conjugate Gradient Method with Guaranteed Descent and an Efficient Line Search”. In: *SIAM Journal on Optimization* 16.1 (2005), pp. 170–192.
- [HZ06] W. W. Hager and H. Zhang. “A survey of nonlinear conjugate gradient methods”. In: *Pacific Journal of Optimization* 2.1 (2006), pp. 35–58.
- [NW06] Jorge Nocedal and Stephen J. Wright. *Numerical Optimization*. second. New York, NY, USA: Springer, 2006.
- [Bor08] Vivek S. Borkar. *Stochastic Approximation: A Dynamical Systems Viewpoint*. Hindustan Book Agency: Springer, 2008.
- [Le+11] Quoc V Le et al. “On optimization methods for deep learning”. In: *ICML*. 2011.
- [Sut+13] I. Sutskever et al. “On the importance of initialization and momentum in deep learning”. In: *International Conference on Machine Learning* (2013), pp. 1139–1147.

⁷<https://abci.ai/>

[Goo+14] Ian Goodfellow et al. “Generative adversarial nets”. In: *Advances in neural information processing systems* 27 (2014).

[KB15] Diederik P. Kingma and Jimmy Ba. “Adam: A Method for Stochastic Optimization”. In: *3rd International Conference on Learning Representations, ICLR 2015, San Diego, CA, USA, May 7-9, 2015, Conference Track Proceedings*. Ed. by Yoshua Bengio and Yann LeCun. 2015. URL: <http://arxiv.org/abs/1412.6980>.

[Mey+15] Simone Meyer et al. “Phase-based frame interpolation for video”. In: *Proceedings of the IEEE conference on computer vision and pattern recognition*. 2015, pp. 1410–1418.

[RMC15] Alec Radford, Luke Metz, and Soumith Chintala. “Unsupervised representation learning with deep convolutional generative adversarial networks”. In: *arXiv preprint arXiv:1511.06434* (2015).

[Pat+16] Deepak Pathak et al. “Context encoders: Feature learning by inpainting”. In: *Proceedings of the IEEE conference on computer vision and pattern recognition*. 2016, pp. 2536–2544.

[Goo17] Ian J. Goodfellow. “NIPS 2016 Tutorial: Generative Adversarial Networks”. In: *CoRR* abs/1701.00160 (2017). arXiv: <1701.00160>. URL: <http://arxiv.org/abs/1701.00160>.

[Heu+17] M. Heusel et al. “GANs Trained by a Two Time-Scale Update Rule Converge to a Local Nash Equilibrium”. In: *International Conference on Neural Information Processing Systems* (2017), pp. 1–12.

[Zha+17] Han Zhang et al. “Stackgan: Text to photo-realistic image synthesis with stacked generative adversarial networks”. In: *Proceedings of the IEEE international conference on computer vision*. 2017, pp. 5907–5915.

[Zhu+17] Jun-Yan Zhu et al. “Unpaired image-to-image translation using cycle-consistent adversarial networks”. In: *Proceedings of the IEEE international conference on computer vision*. 2017, pp. 2223–2232.

[BDS18] Andrew Brock, Jeff Donahue, and Karen Simonyan. “Large scale GAN training for high fidelity natural image synthesis”. In: *arXiv preprint arXiv:1809.11096* (2018).

[DMP18] Chris Donahue, Julian McAuley, and Miller Puckette. “Adversarial audio synthesis”. In: *arXiv preprint arXiv:1802.04208* (2018).

[FGD18] William Fedus, Ian Goodfellow, and Andrew M Dai. “Maskgan: better text generation via filling in the_”. In: *arXiv preprint arXiv:1801.07736* (2018).

[Miy+18] Takeru Miyato et al. “Spectral Normalization for Generative Adversarial Networks”. In: *CoRR* abs/1802.05957 (2018). arXiv: <1802.05957>. URL: <http://arxiv.org/abs/1802.05957>.

[RKK18] Sashank J. Reddi, Satyen Kale, and Sanjiv Kumar. “On the Convergence of Adam and Beyond”. In: *6th International Conference on Learning Representations, ICLR 2018, Vancouver, BC, Canada, April 30 - May 3, 2018, Conference Track Proceedings*. OpenReview.net, 2018. URL: <https://openreview.net/forum?id=ryQu7f-RZ>.

[HAU19] Hideaki Hayashi, Kohtaro Abe, and Seiichi Uchida. “GlyphGAN: Style-consistent font generation based on generative adversarial networks”. In: *Knowledge-Based Systems* 186 (2019), p. 104927.

[KLA19] Tero Karras, Samuli Laine, and Timo Aila. “A style-based generator architecture for generative adversarial networks”. In: *Proceedings of the IEEE/CVF conference on computer vision and pattern recognition*. 2019, pp. 4401–4410.

[San+19] Veit Sandfort et al. “Data augmentation using generative adversarial networks (CycleGAN) to improve generalizability in CT segmentation tasks”. In: *Scientific reports* 9.1 (2019), pp. 1–9.

[Zhu+20] Juntang Zhuang et al. “AdaBelief Optimizer: Adapting Stepsizes by the Belief in Observed Gradients”. In: *Advances in Neural Information Processing Systems 33: Annual Conference on Neural Information Processing Systems 2020, NeurIPS 2020, December 6-12, 2020, virtual*. Ed. by Hugo Larochelle et al. 2020. URL: <https://proceedings.neurips.cc/paper/2020/hash/d9d4f495e875a2e075a1a4a6e1b9770f-Abstract.html>.

Appendix

Unless stated otherwise, all relations between random variables are supported to hold almost surely.

A Lemmas

We prove the following lemma:

Lemma A.1 *Under (A1), (A2), (C3), and (C4), for all $n \in \mathbb{N}$,*

$$\mathbb{E} \left[\|\mathcal{G}(\boldsymbol{\theta}_n, \mathbf{w}_n)\|^2 \right] \leq K_1^2 := \frac{2(C_1 L_1 + \tilde{C}_1)^2}{m^2} + 2B_1^2,$$

where C_1 and \tilde{C}_1 denote upper bounds of $\|\boldsymbol{\theta}_n - \boldsymbol{\theta}\|$ and $\|\mathcal{G}_{\mathbf{w}_n}(\boldsymbol{\theta})\|$ for all $\boldsymbol{\theta} \in \mathbb{R}^\Theta$ and all $n \in \mathbb{N}$, respectively. Additionally, under (C2), we have that, for all $n \in \mathbb{N}$,

$$\mathbb{E} \left[\|\mathbf{d}^G(\boldsymbol{\theta}_n, \mathbf{w}_n)\|^2 \right] \leq 4\tilde{K}_1^2,$$

where $\tilde{K}_1^2 := \max\{K_1^2, \|\mathbf{d}^G(\boldsymbol{\theta}_{-1}, \mathbf{w}_{-1})\|^2\}$.

Proof of Lemma A.1: Let $\boldsymbol{\theta} \in \mathbb{R}^\Theta$ be fixed arbitrarily. Assumption (C4) implies that there exists $C_1 \in \mathbb{R}_{++}$ such that $\sup\{\|\boldsymbol{\theta}_n - \boldsymbol{\theta}\| : n \in \mathbb{N}\} \leq C_1$. Assumption (A2) thus implies that, for all $n \in \mathbb{N}$,

$$\|\mathcal{G}_{\mathbf{w}_n}(\boldsymbol{\theta}_n) - \mathcal{G}_{\mathbf{w}_n}(\boldsymbol{\theta})\| \leq L_1 \|\boldsymbol{\theta}_n - \boldsymbol{\theta}\| \leq C_1 L_1.$$

Assumption (A1) ensures that $\|\mathcal{G}_{(\cdot)}(\boldsymbol{\theta})\| : \mathbb{R}^W \rightarrow \mathbb{R}$ is continuous. Hence, (C4) guarantees that there exists $\tilde{C}_1 \in \mathbb{R}_{++}$ such that $\sup\{\|\mathcal{G}_{\mathbf{w}_n}(\boldsymbol{\theta})\| : n \in \mathbb{N}\} \leq \tilde{C}_1$. The triangle inequality guarantees that, for all $n \in \mathbb{N}$,

$$\|\mathcal{G}_{\mathbf{w}_n}(\boldsymbol{\theta}_n)\| \leq \|\mathcal{G}_{\mathbf{w}_n}(\boldsymbol{\theta}_n) - \mathcal{G}_{\mathbf{w}_n}(\boldsymbol{\theta})\| + \|\mathcal{G}_{\mathbf{w}_n}(\boldsymbol{\theta})\| \leq C_1 L_1 + \tilde{C}_1,$$

which implies that

$$\|\mathcal{G}(\boldsymbol{\theta}_n, \mathbf{w}_n)\|^2 \leq \frac{2}{m^2} \|\mathcal{G}_{\mathbf{w}_n}(\boldsymbol{\theta}_n)\|^2 + 2M^{(\boldsymbol{\theta}_n)^2} \leq \frac{2(C_1 L_1 + \tilde{C}_1)^2}{m^2} + 2M^{(\boldsymbol{\theta}_n)^2}.$$

Accordingly, (C3) ensures that

$$\mathbb{E} \left[\|\mathcal{G}(\boldsymbol{\theta}_n, \mathbf{w}_n)\|^2 \right] \leq \frac{2(C_1 L_1 + \tilde{C}_1)^2}{m^2} + 2B_1^2 =: K_1^2.$$

Let us define $\tilde{K}_1^2 := \max\{K_1^2, \|\mathbf{d}^G(\boldsymbol{\theta}_{-1}, \mathbf{w}_{-1})\|^2\}$. We will use mathematical induction to show that, for all $n \in \mathbb{N}$, $\mathbb{E}[\|\mathbf{d}^G(\boldsymbol{\theta}_n, \mathbf{w}_n)\|^2] \leq 4\tilde{K}_1^2$. When $n = 1$, we have that

$$\begin{aligned} \mathbb{E} \left[\|\mathbf{d}^G(\boldsymbol{\theta}_1, \mathbf{w}_1)\|^2 \right] &\leq 2\mathbb{E} \left[\|\mathcal{G}(\boldsymbol{\theta}_1, \mathbf{w}_1)\|^2 \right] + 2\beta_1^{G^2} \mathbb{E} \left[\|\mathbf{d}^G(\boldsymbol{\theta}_{-1}, \mathbf{w}_{-1})\|^2 \right] \\ &\leq 2K_1^2 + 2 \left(\frac{1}{2} \right)^2 4\tilde{K}_1^2 = 4\tilde{K}_1^2, \end{aligned}$$

where the second inequality comes from the condition $\beta_n^G \in [0, 1/2]$. Assume that $\mathbb{E}[\|\mathbf{d}^G(\boldsymbol{\theta}_n, \mathbf{w}_n)\|^2] \leq 4\tilde{K}_1^2$ for some n . We have that

$$\begin{aligned} \mathbb{E} \left[\|\mathbf{d}^G(\boldsymbol{\theta}_{n+1}, \mathbf{w}_{n+1})\|^2 \right] &\leq 2\mathbb{E} \left[\|\mathcal{G}(\boldsymbol{\theta}_{n+1}, \mathbf{w}_{n+1})\|^2 \right] + 2\beta_n^{G^2} \mathbb{E} \left[\|\mathbf{d}^G(\boldsymbol{\theta}_n, \mathbf{w}_n)\|^2 \right] \\ &\leq 2K_1^2 + 2 \left(\frac{1}{2} \right)^2 4\tilde{K}_1^2 = 4\tilde{K}_1^2. \end{aligned}$$

Hence, we have that, for all $n \in \mathbb{N}$, $\mathbb{E}[\|\mathbf{d}^G(\boldsymbol{\theta}_n, \mathbf{w}_n)\|^2] \leq 4\tilde{K}_1^2$. \square

A discussion similar to the one for showing Lemma A.1 leads to the following lemma.

Lemma A.2 Under (A1), (A2), (C3), and (C4), for all $n \in \mathbb{N}$,

$$\mathbb{E} [\|\mathcal{D}(\boldsymbol{\theta}_n, \mathbf{w}_n)\|^2] \leq K_2^2 := \frac{2(C_2 L_2 + \tilde{C}_2)^2}{m^2} + 2B_2^2,$$

where C_2 and \tilde{C}_2 denote upper bounds of $\|\mathbf{w}_n - \mathbf{w}\|$ and $\|\mathcal{D}_{\boldsymbol{\theta}_n}(\mathbf{w})\|$ for all $\mathbf{w} \in \mathbb{R}^W$ and all $n \in \mathbb{N}$, respectively. Additionally, under (C2), we have that, for all $n \in \mathbb{N}$,

$$\mathbb{E} [\|\mathbf{d}^D(\boldsymbol{\theta}_n, \mathbf{w}_n)\|^2] \leq 4\tilde{K}_2^2,$$

where $\tilde{K}_2^2 := \max\{K_2^2, \|\mathbf{d}^D(\boldsymbol{\theta}_{-1}, \mathbf{w}_{-1})\|^2\}$.

Lemma A.3 Under the assumptions in Lemma A.1, for all $\boldsymbol{\theta} \in \mathbb{R}^\Theta$, all $\mathbf{w} \in \mathbb{R}^W$, and all $n \in \mathbb{N}$,

$$\begin{aligned} \mathbb{E} [\|\boldsymbol{\theta}_{n+1} - \boldsymbol{\theta}\|^2] &\leq \mathbb{E} [\|\boldsymbol{\theta}_n - \boldsymbol{\theta}\|^2] + 2a_n \left(\mathbb{E} [\langle \boldsymbol{\theta} - \boldsymbol{\theta}_n, \nabla_{\boldsymbol{\theta}} \mathcal{L}_G(\boldsymbol{\theta}_n, \mathbf{w}_n) \rangle] + B_1 C_1 + 2C_1 \tilde{K}_1 \beta_n^G \right) + 4\tilde{K}_1^2 a_n^2, \\ \mathbb{E} [\|\mathbf{w}_{n+1} - \mathbf{w}\|^2] &\leq \mathbb{E} [\|\mathbf{w}_n - \mathbf{w}\|^2] + 2b_n \left(\mathbb{E} [\langle \mathbf{w} - \mathbf{w}_n, \nabla_{\mathbf{w}} \mathcal{L}_D(\boldsymbol{\theta}_n, \mathbf{w}_n) \rangle] + B_2 C_2 + 2C_2 \tilde{K}_2 \beta_n^D \right) + 4\tilde{K}_2^2 b_n^2. \end{aligned}$$

Proof of Lemma A.3: Let $\boldsymbol{\theta} \in \mathbb{R}^\Theta$ and $n \in \mathbb{N}$ be fixed arbitrarily. The definition of $\mathbf{d}^G(\boldsymbol{\theta}_n, \mathbf{w}_n)$ ensures that

$$\langle \boldsymbol{\theta}_n - \boldsymbol{\theta}, \mathbf{d}^G(\boldsymbol{\theta}_n, \mathbf{w}_n) \rangle = \langle \boldsymbol{\theta} - \boldsymbol{\theta}_n, \mathcal{G}(\boldsymbol{\theta}_n, \mathbf{w}_n) \rangle + \beta_n^G \langle \boldsymbol{\theta}_n - \boldsymbol{\theta}, \mathbf{d}^G(\boldsymbol{\theta}_{n-1}, \mathbf{w}_{n-1}) \rangle,$$

which, together with the Cauchy–Schwarz inequality and Lemma A.1, implies that

$$\langle \boldsymbol{\theta}_n - \boldsymbol{\theta}, \mathbf{d}^G(\boldsymbol{\theta}_n, \mathbf{w}_n) \rangle \leq \langle \boldsymbol{\theta} - \boldsymbol{\theta}_n, \mathcal{G}(\boldsymbol{\theta}_n, \mathbf{w}_n) \rangle + \beta_n^G C_1 \|\mathbf{d}^G(\boldsymbol{\theta}_{n-1}, \mathbf{w}_{n-1})\|.$$

Accordingly, Lemma A.1 and Jensen's inequality give

$$\mathbb{E} [\langle \boldsymbol{\theta}_n - \boldsymbol{\theta}, \mathbf{d}^G(\boldsymbol{\theta}_n, \mathbf{w}_n) \rangle] \leq \mathbb{E} [\langle \boldsymbol{\theta} - \boldsymbol{\theta}_n, \mathcal{G}(\boldsymbol{\theta}_n, \mathbf{w}_n) \rangle] + 2C_1 \tilde{K}_1 \beta_n^G.$$

From the definition of $\mathcal{G}(\boldsymbol{\theta}_n, \mathbf{w}_n)$, we also have that

$$\begin{aligned} \mathbb{E} [\langle \boldsymbol{\theta} - \boldsymbol{\theta}_n, \mathcal{G}(\boldsymbol{\theta}_n, \mathbf{w}_n) \rangle] &= \frac{1}{m} \mathbb{E} [\langle \boldsymbol{\theta} - \boldsymbol{\theta}_n, \mathcal{G}_{\mathbf{w}_n}(\boldsymbol{\theta}_n) \rangle] + \mathbb{E} [\langle \boldsymbol{\theta} - \boldsymbol{\theta}_n, M^{(\boldsymbol{\theta}_n)} \rangle] \\ &\leq \frac{1}{m} \mathbb{E} [\langle \boldsymbol{\theta} - \boldsymbol{\theta}_n, \mathcal{G}_{\mathbf{w}_n}(\boldsymbol{\theta}_n) \rangle] + B_1 C_1, \end{aligned}$$

where the first inequality comes from the Cauchy–Schwarz inequality and the definitions of B_1 and C_1 . Let us define the independent and identically distributed samples considered here by ξ_0, ξ_1, \dots and denote the history of process ξ_0, ξ_1, \dots to time step n by $\xi_{[n]} := (\xi_0, \xi_1, \dots, \xi_n)$. Accordingly, we have

$$\begin{aligned} \mathbb{E} \left[\left\langle \boldsymbol{\theta} - \boldsymbol{\theta}_n, \frac{1}{m} \mathcal{G}_{\mathbf{w}_n}(\boldsymbol{\theta}_n) \right\rangle \right] &= \mathbb{E} \left[\mathbb{E} \left[\left\langle \boldsymbol{\theta} - \boldsymbol{\theta}_n, \frac{1}{m} \mathcal{G}_{\mathbf{w}_n}(\boldsymbol{\theta}_n) \right\rangle \middle| \xi_{[n]} \right] \right] = \mathbb{E} \left[\left\langle \boldsymbol{\theta} - \boldsymbol{\theta}_n, \mathbb{E} \left[\frac{1}{m} \mathcal{G}_{\mathbf{w}_n}(\boldsymbol{\theta}_n) \middle| \xi_{[n]} \right] \right\rangle \right] \\ &= \mathbb{E} [\langle \boldsymbol{\theta} - \boldsymbol{\theta}_n, \nabla_{\boldsymbol{\theta}} \mathcal{L}_G(\boldsymbol{\theta}_n, \mathbf{w}_n) \rangle]. \end{aligned}$$

Therefore, we have that

$$\mathbb{E} [\langle \boldsymbol{\theta}_n - \boldsymbol{\theta}, \mathbf{d}^G(\boldsymbol{\theta}_n, \mathbf{w}_n) \rangle] \leq \mathbb{E} [\langle \boldsymbol{\theta} - \boldsymbol{\theta}_n, \nabla_{\boldsymbol{\theta}} \mathcal{L}_G(\boldsymbol{\theta}_n, \mathbf{w}_n) \rangle] + B_1 C_1 + 2C_1 \tilde{K}_1 \beta_n^G.$$

The definition of $\boldsymbol{\theta}_{n+1}$ guarantees that

$$\begin{aligned} \|\boldsymbol{\theta}_{n+1} - \boldsymbol{\theta}\|^2 &= \|(\boldsymbol{\theta}_n - \boldsymbol{\theta}) + a_n \mathbf{d}^G(\boldsymbol{\theta}_n, \mathbf{w}_n)\|^2 \\ &= \|\boldsymbol{\theta}_n - \boldsymbol{\theta}\|^2 + 2a_n \langle \boldsymbol{\theta}_n - \boldsymbol{\theta}, \mathbf{d}^G(\boldsymbol{\theta}_n, \mathbf{w}_n) \rangle + a_n^2 \|\mathbf{d}^G(\boldsymbol{\theta}_n, \mathbf{w}_n)\|^2. \end{aligned}$$

Taking the expectation of the above inequality gives

$$\mathbb{E} [\|\boldsymbol{\theta}_{n+1} - \boldsymbol{\theta}\|^2] \leq \mathbb{E} [\|\boldsymbol{\theta}_n - \boldsymbol{\theta}\|^2] + 2a_n \left(\mathbb{E} [\langle \boldsymbol{\theta} - \boldsymbol{\theta}_n, \nabla_{\boldsymbol{\theta}} \mathcal{L}_G(\boldsymbol{\theta}_n, \mathbf{w}_n) \rangle] + B_1 C_1 + 2C_1 \tilde{K}_1 \beta_n^G \right) + 4\tilde{K}_1^2 a_n^2.$$

A discussion similar to the one for showing the above inequality leads to the following inequality:

$$\mathbb{E} [\|\mathbf{w}_{n+1} - \mathbf{w}\|^2] \leq \mathbb{E} [\|\mathbf{w}_n - \mathbf{w}\|^2] + 2b_n \left(\mathbb{E} [\langle \mathbf{w} - \mathbf{w}_n, \nabla_{\mathbf{w}} \mathcal{L}_D(\boldsymbol{\theta}_n, \mathbf{w}_n) \rangle] + B_2 C_2 + 2C_2 \tilde{K}_2 \beta_n^D \right) + 4\tilde{K}_2^2 b_n^2.$$

This completes the proof. \square

B Proofs of Theorems 3.1 and 3.2

Proof of Theorem 3.1: Let $\boldsymbol{\theta} \in \mathbb{R}^\Theta$ and $\mathbf{w} \in \mathbb{R}^W$ be fixed arbitrarily. First, we show that, for all $\epsilon > 0$,

$$\liminf_{n \rightarrow +\infty} \mathbb{E} [\langle \boldsymbol{\theta}_n - \boldsymbol{\theta}, \nabla_{\boldsymbol{\theta}} \mathcal{L}_G(\boldsymbol{\theta}_n, \mathbf{w}_n) \rangle] \leq 2\tilde{K}_1^2 a + 2C_1\tilde{K}_1\beta^G + B_1C_1 + \epsilon. \quad (28)$$

If (28) does not hold, then there exists $\epsilon_0 > 0$ such that

$$\liminf_{n \rightarrow +\infty} \mathbb{E} [\langle \boldsymbol{\theta}_n - \boldsymbol{\theta}, \nabla_{\boldsymbol{\theta}} \mathcal{L}_G(\boldsymbol{\theta}_n, \mathbf{w}_n) \rangle] > 2\tilde{K}_1^2 a + 2C_1\tilde{K}_1\beta^G + B_1C_1 + \epsilon_0.$$

Since there exists $n_0 \in \mathbb{N}$ such that, for all $n \geq n_0$,

$$\liminf_{n \rightarrow +\infty} \mathbb{E} [\langle \boldsymbol{\theta}_n - \boldsymbol{\theta}, \nabla_{\boldsymbol{\theta}} \mathcal{L}_G(\boldsymbol{\theta}_n, \mathbf{w}_n) \rangle] - \frac{\epsilon_0}{2} \leq \mathbb{E} [\langle \boldsymbol{\theta}_n - \boldsymbol{\theta}, \nabla_{\boldsymbol{\theta}} \mathcal{L}_G(\boldsymbol{\theta}_n, \mathbf{w}_n) \rangle],$$

we have that, for all $n \geq n_0$,

$$\mathbb{E} [\langle \boldsymbol{\theta}_n - \boldsymbol{\theta}, \nabla_{\boldsymbol{\theta}} \mathcal{L}_G(\boldsymbol{\theta}_n, \mathbf{w}_n) \rangle] > 2\tilde{K}_1^2 a + 2C_1\tilde{K}_1\beta^G + B_1C_1 + \frac{\epsilon_0}{2}.$$

Lemma A.3, together with (C1) and (C2), ensures that, for all $n \in \mathbb{N}$,

$$\begin{aligned} \mathbb{E} [\|\boldsymbol{\theta}_{n+1} - \boldsymbol{\theta}\|^2] &\leq \mathbb{E} [\|\boldsymbol{\theta}_n - \boldsymbol{\theta}\|^2] + 2a \left(\mathbb{E} [\langle \boldsymbol{\theta} - \boldsymbol{\theta}_n, \nabla_{\boldsymbol{\theta}} \mathcal{L}_G(\boldsymbol{\theta}_n, \mathbf{w}_n) \rangle] + B_1C_1 + 2C_1\tilde{K}_1\beta^G \right) \\ &\quad + 4\tilde{K}_1^2 a^2. \end{aligned} \quad (29)$$

Accordingly, for all $n \geq n_0$,

$$\begin{aligned} \mathbb{E} [\|\boldsymbol{\theta}_{n+1} - \boldsymbol{\theta}\|^2] &< \mathbb{E} [\|\boldsymbol{\theta}_n - \boldsymbol{\theta}\|^2] - 2a \left(2\tilde{K}_1^2 a + 2C_1\tilde{K}_1\beta^G + B_1C_1 + \frac{\epsilon_0}{2} \right) + 2aB_1C_1 + 4aC_1\tilde{K}_1\beta^G + 4\tilde{K}_1^2 a^2 \\ &= \mathbb{E} [\|\boldsymbol{\theta}_n - \boldsymbol{\theta}\|^2] - a\epsilon_0 \\ &< \mathbb{E} [\|\boldsymbol{\theta}_{n_0} - \boldsymbol{\theta}\|^2] - a\epsilon_0(n + 1 - n_0). \end{aligned}$$

$\mathbb{E} [\|\boldsymbol{\theta}_{n_0} - \boldsymbol{\theta}\|^2] - a\epsilon_0(n + 1 - n_0)$ approaches minus infinity as n approaches positive infinity. This is a contradiction. Hence, (28) holds. Since $\epsilon > 0$ is arbitrary, we have that

$$\liminf_{n \rightarrow +\infty} \mathbb{E} [\langle \boldsymbol{\theta}_n - \boldsymbol{\theta}, \nabla_{\boldsymbol{\theta}} \mathcal{L}_G(\boldsymbol{\theta}_n, \mathbf{w}_n) \rangle] \leq 2\tilde{K}_1^2 a + 2C_1\tilde{K}_1\beta^G + B_1C_1. \quad (30)$$

A discussion similar to the one for showing the above inequality leads to the following inequality:

$$\liminf_{n \rightarrow +\infty} \mathbb{E} [\langle \mathbf{w}_n - \mathbf{w}, \nabla_{\mathbf{w}} \mathcal{L}_D(\boldsymbol{\theta}_n, \mathbf{w}_n) \rangle] \leq 2\tilde{K}_2^2 b + 2C_2\tilde{K}_2\beta^D + B_2C_2. \quad (31)$$

Inequality (30) ensures that there exists a subsequence $((\boldsymbol{\theta}_{n_i}, \mathbf{w}_{n_i}))_{i \in \mathbb{N}}$ of $((\boldsymbol{\theta}_n, \mathbf{w}_n))_{n \in \mathbb{N}}$ such that, for all $\boldsymbol{\theta} \in \mathbb{R}^\Theta$,

$$\lim_{i \rightarrow +\infty} \mathbb{E} [\langle \boldsymbol{\theta}_{n_i} - \boldsymbol{\theta}, \nabla_{\boldsymbol{\theta}} \mathcal{L}_G(\boldsymbol{\theta}_{n_i}, \mathbf{w}_{n_i}) \rangle] = \liminf_{n \rightarrow +\infty} \mathbb{E} [\langle \boldsymbol{\theta}_n - \boldsymbol{\theta}, \nabla_{\boldsymbol{\theta}} \mathcal{L}_G(\boldsymbol{\theta}_n, \mathbf{w}_n) \rangle] \leq 2\tilde{K}_1^2 a + 2C_1\tilde{K}_1\beta^G + B_1C_1.$$

Assumption (C4) implies that there exists $((\boldsymbol{\theta}_{n_j}, \mathbf{w}_{n_j}))_{j \in \mathbb{N}}$ of $((\boldsymbol{\theta}_n, \mathbf{w}_n))_{n \in \mathbb{N}}$ such that $((\boldsymbol{\theta}_{n_j}, \mathbf{w}_{n_j}))_{j \in \mathbb{N}}$ converges almost surely to $(\boldsymbol{\theta}^*, \mathbf{w}^*)$. Accordingly, for all $\boldsymbol{\theta} \in \mathbb{R}^\Theta$,

$$\mathbb{E} [\langle \boldsymbol{\theta}^* - \boldsymbol{\theta}, \nabla_{\boldsymbol{\theta}} \mathcal{L}_G(\boldsymbol{\theta}^*, \mathbf{w}^*) \rangle] \leq 2\tilde{K}_1^2 a + 2C_1\tilde{K}_1\beta^G + B_1C_1,$$

which implies that

$$\mathbb{E} [\|\nabla_{\boldsymbol{\theta}} \mathcal{L}_G(\boldsymbol{\theta}^*, \mathbf{w}^*)\|^2] \leq 2\tilde{K}_1^2 a + 2C_1\tilde{K}_1\beta^G + B_1C_1. \quad (32)$$

A discussion similar to the one for showing the above inequality, together with (31), means that there exists a subsequence $((\boldsymbol{\theta}_{n_k}, \mathbf{w}_{n_k}))_{k \in \mathbb{N}}$ of $((\boldsymbol{\theta}_n, \mathbf{w}_n))_{n \in \mathbb{N}}$ such that $((\boldsymbol{\theta}_{n_k}, \mathbf{w}_{n_k}))_{k \in \mathbb{N}}$ converges almost surely to $(\boldsymbol{\theta}_*, \mathbf{w}_*)$ satisfying

$$\mathbb{E} [\|\nabla_{\mathbf{w}} \mathcal{L}_D(\boldsymbol{\theta}_*, \mathbf{w}_*)\|^2] \leq 2\tilde{K}_2^2 b + 2C_2\tilde{K}_2\beta^D + B_2C_2. \quad (33)$$

Inequality (29) implies that

$$\mathbb{E} [\langle \boldsymbol{\theta}_n - \boldsymbol{\theta}, \nabla_{\boldsymbol{\theta}} \mathcal{L}_G(\boldsymbol{\theta}_n, \mathbf{w}_n) \rangle] \leq \frac{1}{2a} \left\{ \mathbb{E} [\|\boldsymbol{\theta}_n - \boldsymbol{\theta}\|^2] - \mathbb{E} [\|\boldsymbol{\theta}_{n+1} - \boldsymbol{\theta}\|^2] \right\} + 2\tilde{K}_1^2 a + B_1 C_1 + 2C_1 \tilde{K}_1 \beta_n^G.$$

Summing the above inequality from $n = 1$ to $n = N$ guarantees that

$$\begin{aligned} & \sum_{n \in [N]} \mathbb{E} [\langle \boldsymbol{\theta}_n - \boldsymbol{\theta}, \nabla_{\boldsymbol{\theta}} \mathcal{L}_G(\boldsymbol{\theta}_n, \mathbf{w}_n) \rangle] \\ & \leq \frac{1}{2a} \left\{ \mathbb{E} [\|\boldsymbol{\theta}_1 - \boldsymbol{\theta}\|^2] - \mathbb{E} [\|\boldsymbol{\theta}_{N+1} - \boldsymbol{\theta}\|^2] \right\} + 2\tilde{K}_1^2 N a + B_1 C_1 N + 2C_1 \tilde{K}_1 \sum_{n \in [N]} \beta_n^G \\ & \leq \frac{1}{2a} \mathbb{E} [\|\boldsymbol{\theta}_1 - \boldsymbol{\theta}\|^2] + 2\tilde{K}_1^2 N a + B_1 C_1 N + 2C_1 \tilde{K}_1 \sum_{n \in [N]} \beta_n^G, \end{aligned}$$

which implies that

$$\frac{1}{N} \sum_{n \in [N]} \mathbb{E} [\langle \boldsymbol{\theta}_n - \boldsymbol{\theta}, \nabla_{\boldsymbol{\theta}} \mathcal{L}_G(\boldsymbol{\theta}_n, \mathbf{w}_n) \rangle] \leq \frac{1}{2aN} \mathbb{E} [\|\boldsymbol{\theta}_1 - \boldsymbol{\theta}\|^2] + 2\tilde{K}_1^2 a + B_1 C_1 + \frac{2C_1 \tilde{K}_1}{N} \sum_{n \in [N]} \beta_n^G. \quad (34)$$

A discussion similar to the one for showing (34) leads to the following inequalities:

$$\frac{1}{N} \sum_{n \in [N]} \mathbb{E} [\langle \mathbf{w}_n - \mathbf{w}, \nabla_{\mathbf{w}} \mathcal{L}_D(\boldsymbol{\theta}_n, \mathbf{w}_n) \rangle] \leq \frac{1}{2bN} \mathbb{E} [\|\mathbf{w}_1 - \mathbf{w}\|^2] + 2\tilde{K}_2^2 b + B_2 C_2 + \frac{2C_2 \tilde{K}_2}{N} \sum_{n \in [N]} \beta_n^D.$$

Let us consider the case where $((\boldsymbol{\theta}_n, \mathbf{w}_n))_{n \in \mathbb{N}}$ converges almost surely to $(\boldsymbol{\theta}^*, \mathbf{w}^*)$. Inequalities (32) and (33) indicate that

$$\begin{aligned} \mathbb{E} [\|\nabla_{\boldsymbol{\theta}} \mathcal{L}_G(\boldsymbol{\theta}^*, \mathbf{w}^*)\|^2] & \leq 2\tilde{K}_1^2 a + 2C_1 \tilde{K}_1 \beta^G + B_1 C_1, \\ \mathbb{E} [\|\nabla_{\mathbf{w}} \mathcal{L}_D(\boldsymbol{\theta}^*, \mathbf{w}^*)\|^2] & \leq 2\tilde{K}_2^2 b + 2C_2 \tilde{K}_2 \beta^D + B_2 C_2, \end{aligned}$$

which completes the proof. \square

Proof of Theorem 3.2: (i) The definitions of $\boldsymbol{\theta}_{n+1}$ and \mathbf{w}_{n+1} imply that, for all $n \in \mathbb{N}$,

$$\begin{aligned} \boldsymbol{\theta}_{n+1} &= \boldsymbol{\theta}_n - b_n \frac{a_n}{b_n} \mathcal{G}(\boldsymbol{\theta}_n, \mathbf{w}_n) + a_n \beta_n^G \mathbf{d}^G(\boldsymbol{\theta}_{n-1}, \mathbf{w}_{n-1}), \\ \mathbf{w}_{n+1} &= \mathbf{w}_n - b_n \mathcal{D}(\boldsymbol{\theta}_n, \mathbf{w}_n) + b_n \beta_n^D \mathbf{d}^D(\boldsymbol{\theta}_{n-1}, \mathbf{w}_{n-1}). \end{aligned} \quad (35)$$

Lemma A.1, together with (D3), ensures that $(\|\mathcal{G}(\boldsymbol{\theta}_n, \mathbf{w}_n)\|)_{n \in \mathbb{N}}$, $(\|\mathcal{D}(\boldsymbol{\theta}_n, \mathbf{w}_n)\|)_{n \in \mathbb{N}}$, $(\mathbf{d}^G(\boldsymbol{\theta}_n, \mathbf{w}_n))_{n \in \mathbb{N}}$, and $(\mathbf{d}^D(\boldsymbol{\theta}_n, \mathbf{w}_n))_{n \in \mathbb{N}}$ are almost surely bounded. Assumption 3.2(D1) ensures that (35) can be regarded as a discretized version of the ordinary differential equations $\dot{\mathbf{x}}(t) = \mathbf{0}$ and $\dot{\mathbf{y}}(t) = \mathcal{D}(\mathbf{x}(t), \mathbf{y}(t))$ with a step size b_n and errors at the n -th iteration defined by

$$-\frac{a_n}{b_n} \mathcal{G}(\boldsymbol{\theta}_n, \mathbf{w}_n) + a_n \beta_n^G \mathbf{d}^G(\boldsymbol{\theta}_{n-1}, \mathbf{w}_{n-1}) \text{ and } b_n \beta_n^D \mathbf{d}^D(\boldsymbol{\theta}_{n-1}, \mathbf{w}_{n-1}). \quad (36)$$

Assumptions 3.1(C2) and 3.2(D2)(i) thus guarantee that two sequences defined by (36) converge almost surely to zero. Hence, an argument similar to the one proving Theorem 1.1 in [Bor97] (see [Bor97, Section 2] for the details of the proof) leads to Theorem 3.2(i).

(ii) Lemma A.3 guarantees that, for all $\boldsymbol{\theta} \in \mathbb{R}^\Theta$ and all $n \in \mathbb{N}$,

$$\mathbb{E} [\langle \boldsymbol{\theta}_n - \boldsymbol{\theta}, \nabla_{\boldsymbol{\theta}} \mathcal{L}_G(\boldsymbol{\theta}_n, \mathbf{w}_n) \rangle] \leq \frac{1}{2a_n} \left\{ \mathbb{E} [\|\boldsymbol{\theta}_n - \boldsymbol{\theta}\|^2] - \mathbb{E} [\|\boldsymbol{\theta}_{n+1} - \boldsymbol{\theta}\|^2] \right\} + B_1 C_1 + 2C_1 \tilde{K}_1 \beta_n^G + 2\tilde{K}_1^2 a_n.$$

Summing the above inequality from $n = 1$ to $n = N$ gives, for all $\boldsymbol{\theta} \in \mathbb{R}^\Theta$,

$$\begin{aligned} & \sum_{n \in [N]} \mathbb{E} [\langle \boldsymbol{\theta}_n - \boldsymbol{\theta}, \nabla_{\boldsymbol{\theta}} \mathcal{L}_G(\boldsymbol{\theta}_n, \mathbf{w}_n) \rangle] \\ & \leq \sum_{n \in [N]} \frac{1}{2a_n} \left\{ \mathbb{E} [\|\boldsymbol{\theta}_n - \boldsymbol{\theta}\|^2] - \mathbb{E} [\|\boldsymbol{\theta}_{n+1} - \boldsymbol{\theta}\|^2] \right\} + B_1 C_1 N + 2C_1 \tilde{K}_1 \sum_{n \in [N]} \beta_n^G + 2\tilde{K}_1^2 \sum_{n \in [N]} a_n. \end{aligned}$$

We have that

$$\begin{aligned}
& \sum_{n \in [N]} \frac{1}{a_n} \left\{ \mathbb{E} [\|\boldsymbol{\theta}_n - \boldsymbol{\theta}\|^2] - \mathbb{E} [\|\boldsymbol{\theta}_{n+1} - \boldsymbol{\theta}\|^2] \right\} \\
&= \frac{\mathbb{E} [\|\boldsymbol{\theta}_1 - \boldsymbol{\theta}\|^2]}{a_1} + \sum_{k=2}^N \left\{ \frac{\mathbb{E} [\|\boldsymbol{\theta}_k - \boldsymbol{\theta}\|^2]}{a_k} - \frac{\mathbb{E} [\|\boldsymbol{\theta}_{k-1} - \boldsymbol{\theta}\|^2]}{a_{k-1}} \right\} - \frac{\mathbb{E} [\|\boldsymbol{\theta}_{N+1} - \boldsymbol{\theta}\|^2]}{a_N} \\
&\leq \frac{\mathbb{E} [\|\boldsymbol{\theta}_1 - \boldsymbol{\theta}\|^2]}{a_1} + \mathbb{E} \left[\sum_{k=2}^N \sum_{i \in [\Theta]} \left(\frac{1}{a_k} - \frac{1}{a_{k-1}} \right) (\theta_{k,i} - \theta_i)^2 \right].
\end{aligned}$$

Since $(a_n)_{n \in \mathbb{N}}$ is monotone decreasing, we have that, for all $k \geq 1$, $a_k^{-1} - a_{k-1}^{-1} \geq 0$. Moreover, for all $k \in \mathbb{N}$, $\sum_{i \in [\Theta]} (\theta_{k,i} - \theta_i)^2 \leq \|\boldsymbol{\theta}_k - \boldsymbol{\theta}\|^2 \leq C_1^2$. Hence,

$$\sum_{n \in [N]} \frac{1}{a_n} \left\{ \mathbb{E} [\|\boldsymbol{\theta}_n - \boldsymbol{\theta}\|^2] - \mathbb{E} [\|\boldsymbol{\theta}_{n+1} - \boldsymbol{\theta}\|^2] \right\} \leq \frac{C_1^2}{a_1} + C_1^2 \left(\frac{1}{a_N} - \frac{1}{a_1} \right) = \frac{C_1^2}{a_N}.$$

Therefore, for all $\boldsymbol{\theta} \in \mathbb{R}^\Theta$ and all $N \geq 1$,

$$\frac{1}{N} \sum_{n \in [N]} \mathbb{E} [\langle \boldsymbol{\theta}_n - \boldsymbol{\theta}, \nabla_{\boldsymbol{\theta}} \mathcal{L}_G(\boldsymbol{\theta}_n, \mathbf{w}_n) \rangle] \leq \frac{C_1^2}{2a_N N} + B_1 C_1 + \frac{2C_1 \tilde{K}_1}{N} \sum_{n \in [N]} \beta_n^G + \frac{2\tilde{K}_1^2}{N} \sum_{n \in [N]} a_n.$$

A discussion similar to the one for showing the above inequality leads to the following: for all $\mathbf{w} \in \mathbb{R}^W$ and all $N \geq 1$,

$$\frac{1}{N} \sum_{n \in [N]} \mathbb{E} [\langle \mathbf{w}_n - \mathbf{w}, \nabla_{\mathbf{w}} \mathcal{L}_D(\boldsymbol{\theta}_n, \mathbf{w}_n) \rangle] \leq \frac{C_2^2}{2b_N N} + B_2 C_2 + \frac{2C_2 \tilde{K}_2}{N} \sum_{n \in [N]} \beta_n^D + \frac{2\tilde{K}_2^2}{N} \sum_{n \in [N]} b_n.$$

Let us define $\alpha_n := n^{-\eta}$, where $\eta \in (0, 1)$. Then, we have

$$\frac{1}{\alpha_N N} = \frac{1}{N^{1-\eta}}$$

and

$$\frac{1}{N} \sum_{n \in [N]} \alpha_n \leq \frac{1}{N} \left\{ 1 + \int_1^N \frac{dt}{t^\eta} \right\} \leq \frac{1}{N} \frac{N^{1-\eta}}{1-\eta} = \frac{1}{(1-\eta)N^\eta}.$$

Theorem 3.2(ii) thus leads to

$$\begin{aligned}
& \frac{1}{N} \sum_{n \in [N]} \mathbb{E} [\langle \boldsymbol{\theta}_n - \boldsymbol{\theta}, \nabla_{\boldsymbol{\theta}} \mathcal{L}_G(\boldsymbol{\theta}_n, \mathbf{w}_n) \rangle] \leq \mathcal{O} \left(\frac{1}{N^{\mu_a}} \right) + B_1 C_1, \\
& \frac{1}{N} \sum_{n \in [N]} \mathbb{E} [\langle \mathbf{w}_n - \mathbf{w}, \nabla_{\mathbf{w}} \mathcal{L}_D(\boldsymbol{\theta}_n, \mathbf{w}_n) \rangle] \leq \mathcal{O} \left(\frac{1}{N^{\mu_b}} \right) + B_2 C_2,
\end{aligned}$$

where $\mu_a := \min\{\eta_a, 1 - \eta_a\}$ and $\mu_b := \min\{\eta_b, 1 - \eta_b\}$. This completes the proof. \square

C Experimental Settings

C.1 Implementation and Environment for Experiment

We performed our experiment on ABCI (AI Bridging Cloud Infrastructure), a supercomputer owned by the National Institute of Advanced Industrial Science and Technology. Each node of ABCI is composed of NVIDIA Tesla V100×4GPU and Intel Xeon Gold 6148 2.4 GHz, 20 Cores×2CPU. As a software environment, we use Red Hat 4.8.5, gcc 7.4, Python 3.6.5, Pytorch 1.6.0, cuDNN 7.6.2, and CUDA 10.0.

C.2 Model and datasets

The SNGAN in our experiment basically had the structure of the GAN in Table 1 of [Zhu+20]. However, due to the Lipschitz constraint, the BN of the discriminator was replaced by the SN. We used MNIST and CIFAR10 as datasets. The workload for each experimental setup is shown in Table 6.

Table 6: Workloads

Model	Dataset	Dataset Size	Step Budget
SNGAN [Zhu+20]	MNIST	60000	100K
SNGAN [Zhu+20]	CIFAR10	50000	100K

C.3 Hyperparameters and detailed configuration

C.3.1 Toy example experiments

The hyperparameters of the figures shown in Figure 2 of Section 4.2 are explained here. A momentum coefficient of 0.9 was used for momentum SGD, and FR was set as a beta update for the CG method. Each optimizer had a learning rate to update x and a learning rate to update y . For the constant learning rate settings, we set $3.75e - 08$ as the learning rate of x and $1e - 06$ as the learning rate of y in SGD. Moreover, we set $3.75e - 08$ and $1e - 07$ in the momentum SGD and $2.5e - 08$ and $5e - 07$ in the CG method. The number of steps was 400. After updating x , the gradient of y was updated for the objective function, which used the updated x .

C.3.2 Real-world data experiments

Here, we report the hyperparameter's search space. For the vanilla SGD, we only searched the learning rate η and batch size B . For the non-adaptive momentum methods, was added a fixed value of 0.9 as a parameter to control the momentum γ .

As for the diminishing learning rates, we performed experiments with the center learning rate shown in Table 1 set as the inverse square learning rate. In this case, the current number of steps is n , and the learning rate is adjusted so that it becomes the product of the initial learning rate and $1/\sqrt{n}$. The learning schedule in the most right column of Table 1 was not tested because it corresponds to the inverse square learning rate when $\eta_a = \eta_b = 0.5$.

The change in learning rate at 100K steps for an initial learning rate of 1 is shown in Figure 5.

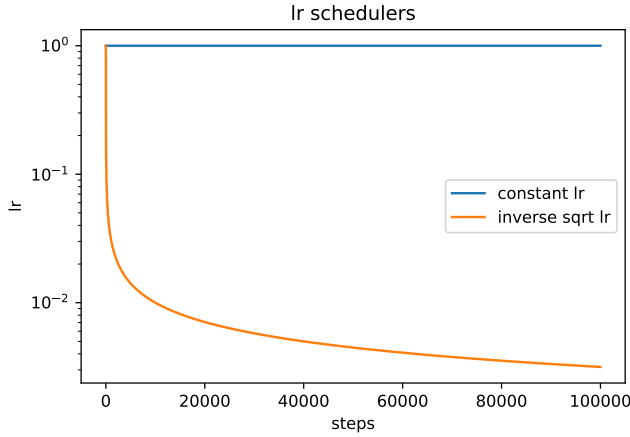


Figure 5. Two types of learning rate scheduler: constant learning rate and inverse square learning rate

Table 7: Hyperparameter Search Range: MNIST SNGAN

Optimizer	β	Update Rule	B	a^1 (Learning rate for Generator)	b^2 (Learning rate for Discriminator)	Learning rate Scheduler Type
SGD	-		{256}	{5e-5, 1e-4, 5e-4. 1e-3, 5e-3}	{5e-5, 1e-4, 5e-4. 1e-3, 5e-3}	{Constant, Inverse Sqrt}
Momentum SGD	-		{256}	{5e-5, 1e-4, 5e-4. 1e-3, 5e-3}	{5e-5, 1e-4, 5e-4. 1e-3, 5e-3}	{Constant, Inverse Sqrt}
Adam	-		{256}	{5e-5, 1e-4, 5e-4. 1e-3, 5e-3}	{5e-5, 1e-4, 5e-4. 1e-3, 5e-3}	{Constant, Inverse Sqrt}
CG	FR		{256}	{5e-5, 1e-4, 5e-4. 1e-3, 5e-3}	{5e-5, 1e-4, 5e-4. 1e-3, 5e-3}	{Constant, Inverse Sqrt}
CG	PRP		{256}	{5e-5, 1e-4, 5e-4. 1e-3, 5e-3}	{5e-5, 1e-4, 5e-4. 1e-3, 5e-3}	{Constant, Inverse Sqrt}
CG	HS		{256}	{5e-5, 1e-4, 5e-4. 1e-3, 5e-3}	{5e-5, 1e-4, 5e-4. 1e-3, 5e-3}	{Constant, Inverse Sqrt}
CG	DY		{256}	{5e-5, 1e-4, 5e-4. 1e-3, 5e-3}	{5e-5, 1e-4, 5e-4. 1e-3, 5e-3}	{Constant, Inverse Sqrt}
CG	HZ		{256}	{5e-5, 1e-4, 5e-4. 1e-3, 5e-3}	{5e-5, 1e-4, 5e-4. 1e-3, 5e-3}	{Constant, Inverse Sqrt}
CG	Hyb1 (HS, DY)		{256}	{5e-5, 1e-4, 5e-4. 1e-3, 5e-3}	{5e-5, 1e-4, 5e-4. 1e-3, 5e-3}	{Constant, Inverse Sqrt}
CG	Hyb2 (FR, PRP)		{256}	{5e-5, 1e-4, 5e-4. 1e-3, 5e-3}	{5e-5, 1e-4, 5e-4. 1e-3, 5e-3}	{Constant, Inverse Sqrt}

Table 8: Hyperparameter Search Range: CIFAR10 SNGAN

Optimizer	β	Update Rule	B	a^1 (Learning rate for Generator)	b^2 (Learning rate for Discriminator)	Learning rate Scheduler Type
SGD	-		{256}	{5e-5, 1e-4, 5e-4. 1e-3, 5e-3}	{5e-5, 1e-4, 5e-4. 1e-3, 5e-3}	{Constant, Inverse Sqrt}
Momentum SGD	-		{256}	{5e-5, 1e-4, 5e-4. 1e-3, 5e-3}	{5e-5, 1e-4, 5e-4. 1e-3, 5e-3}	{Constant, Inverse Sqrt}
Adam	-		{256}	{5e-5, 1e-4, 5e-4. 1e-3, 5e-3}	{5e-5, 1e-4, 5e-4. 1e-3, 5e-3}	{Constant, Inverse Sqrt}
CG	FR		{256}	{5e-5, 1e-4, 5e-4. 1e-3, 5e-3}	{5e-5, 1e-4, 5e-4. 1e-3, 5e-3}	{Constant, Inverse Sqrt}
CG	PRP		{256}	{5e-5, 1e-4, 5e-4. 1e-3, 5e-3}	{5e-5, 1e-4, 5e-4. 1e-3, 5e-3}	{Constant, Inverse Sqrt}
CG	HS		{256}	{5e-5, 1e-4, 5e-4. 1e-3, 5e-3}	{5e-5, 1e-4, 5e-4. 1e-3, 5e-3}	{Constant, Inverse Sqrt}
CG	DY		{256}	{5e-5, 1e-4, 5e-4. 1e-3, 5e-3}	{5e-5, 1e-4, 5e-4. 1e-3, 5e-3}	{Constant, Inverse Sqrt}
CG	HZ		{256}	{5e-5, 1e-4, 5e-4. 1e-3, 5e-3}	{5e-5, 1e-4, 5e-4. 1e-3, 5e-3}	{Constant, Inverse Sqrt}
CG	Hyb1 (HS, DY)		{256}	{5e-5, 1e-4, 5e-4. 1e-3, 5e-3}	{5e-5, 1e-4, 5e-4. 1e-3, 5e-3}	{Constant, Inverse Sqrt}
CG	Hyb2 (FR, PRP)		{256}	{5e-5, 1e-4, 5e-4. 1e-3, 5e-3}	{5e-5, 1e-4, 5e-4. 1e-3, 5e-3}	{Constant, Inverse Sqrt}

¹ a : Initial learning rate for generator
² b : Initial learning rate for discriminator

D Supplemental Experimental Results

D.1 Constant learning rate experiments

Here, we show the loss (Figure 6) and norm of the gradient (Figure 7) for the inverse sqrt learning rate that were omitted from Section 4.3.1.

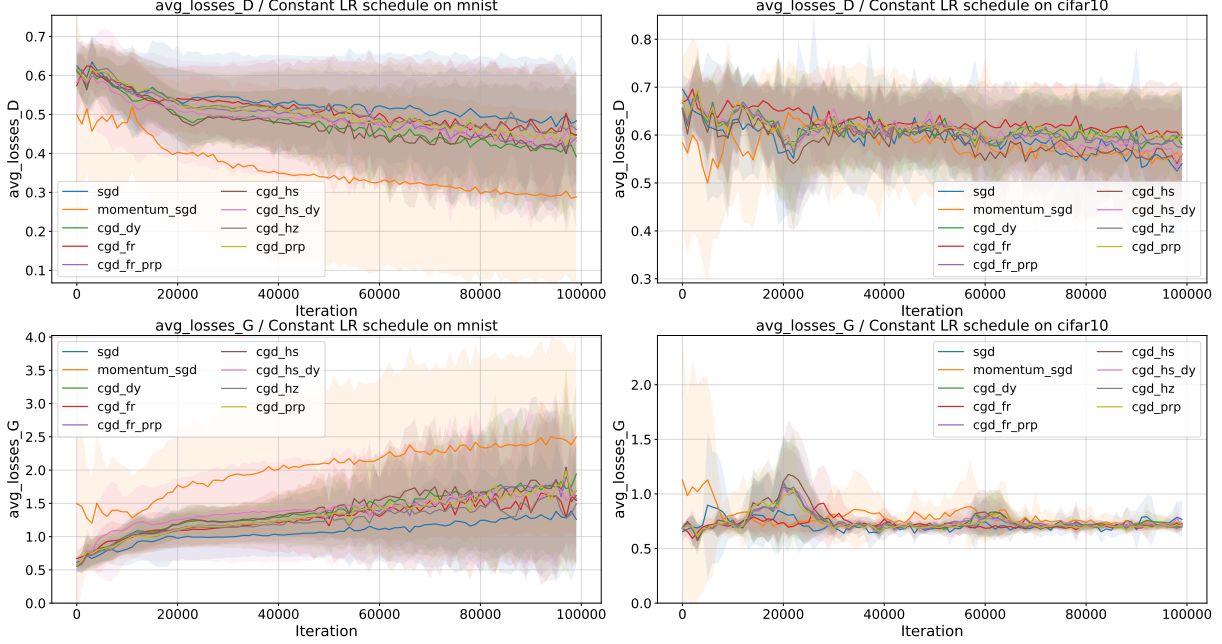


Figure 6. Mean loss (solid line surrounded by the shaded areas) bounded by the maximum and minimum over the best ten runs in sense of FID. **Top Left:** MNIST discriminator loss, **Top Right:** CIFAR-10 discriminator loss, **Bottom Left:** MNIST generator loss, **Bottom Right:** CIFAR-10 generator loss

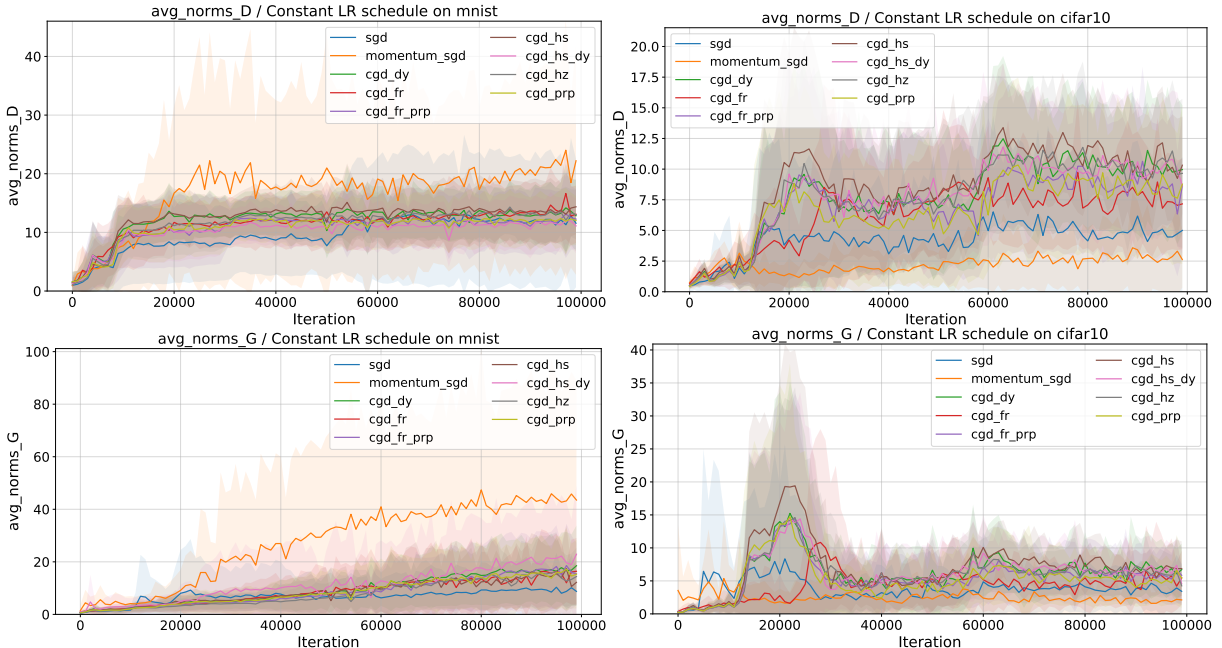


Figure 7. Mean norm of gradient (solid line surrounded by the shaded areas) bounded by the maximum and minimum over the best ten runs in sense of FID. **Top Left:** MNIST discriminator, **Top Right:** CIFAR-10 discriminator, **Bottom Left:** MNIST generator, **Bottom Right:** CIFAR-10 generator

D.2 Diminishing learning rate experiments

Here, we show the loss and norm of the gradient (Figure 8 and 9) experiments with an inverse sqrt learning rate that were omitted from Section 4.3.2.

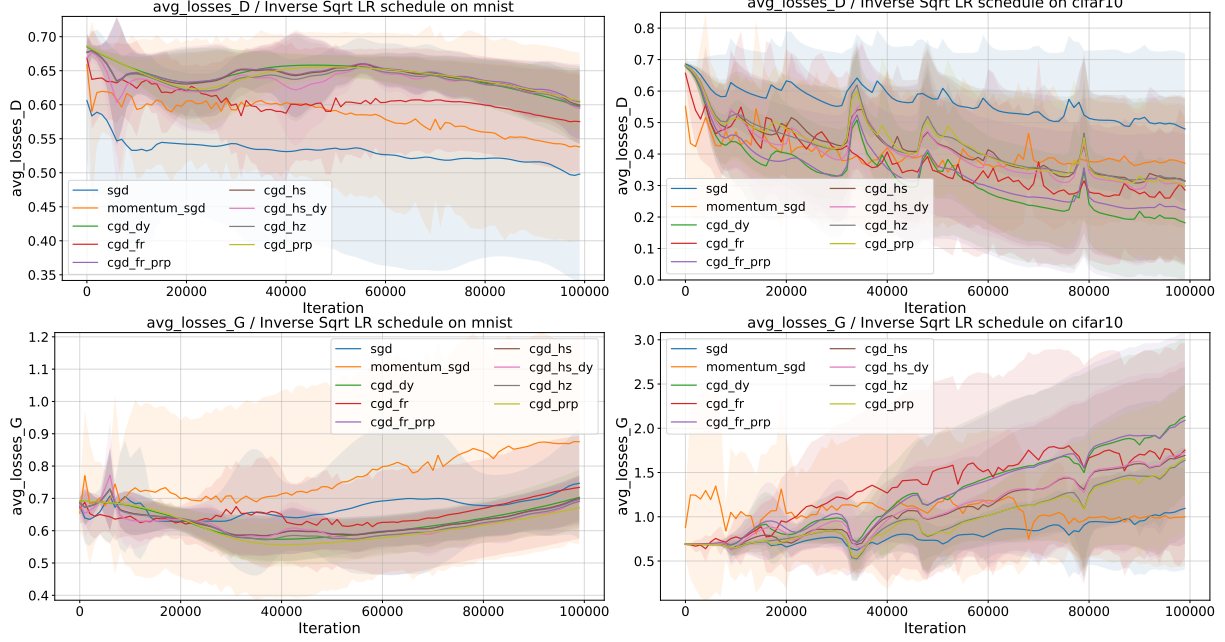


Figure 8. Mean loss (solid line surrounded by the shaded areas) bounded by the maximum and minimum over the best ten runs in sense of FID. **Top Left:** MNIST discriminator loss, **Top Right:** CIFAR-10 discriminator loss, **Bottom Left:** MNIST generator loss, **Bottom Right:** CIFAR-10 generator loss

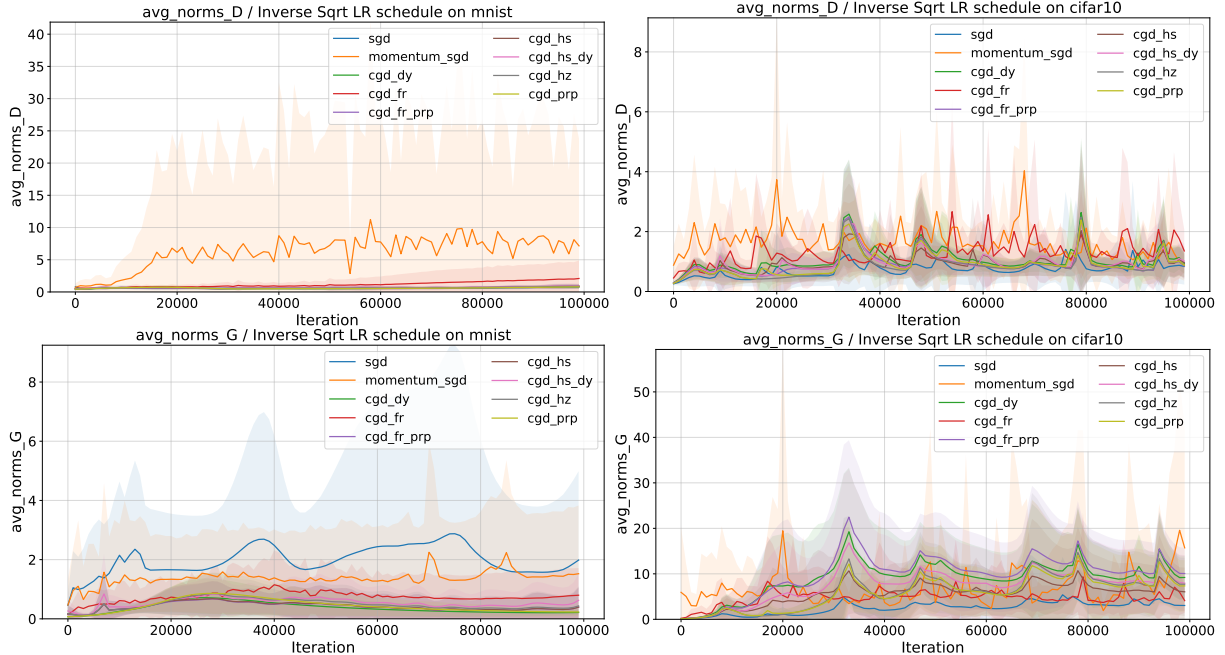


Figure 9. Mean norm of gradient (solid line surrounded by the shaded areas) bounded by the maximum and minimum over the best ten runs in sense of FID. **Top Left:** MNIST discriminator, **Top Right:** CIFAR-10 discriminator, **Bottom Left:** MNIST generator, **Bottom Right:** CIFAR-10 generator

E Additional Experiments

E.1 Sensitivity on learning rate

For all LR schedule \times dataset \times optimizer combinations (36 experimental settings), we performed a grid search of 25 hyperparameter combinations, including six combinations each for LR_G (initial learning rate for generator) and LR_D (initial learning rate for discriminator) and three combinations for batch size. To evaluate the optimizer's performance on LR_G and LR_D, we created a heat map of FID scores.

E.1.1 Constant learning rate

As for the sensitivity to the learning rate, in simple cases like MNIST, momentum SGD shows the most robust performance. Although the SGD and CG methods were slightly inferior to momentum SGD, a common trend was that setting a larger learning rate for the generator gave a better FID score.

In the CIFAR10 case, which is a more complicated problem setting, momentum SGD performed poorly overall, while the CG methods performed the best in the sense of FID but suffered from sensitivity that led to them having the worst FID score when the learning rate of the discriminator was multiplied by 5 (SGD did not suffer from this problem).

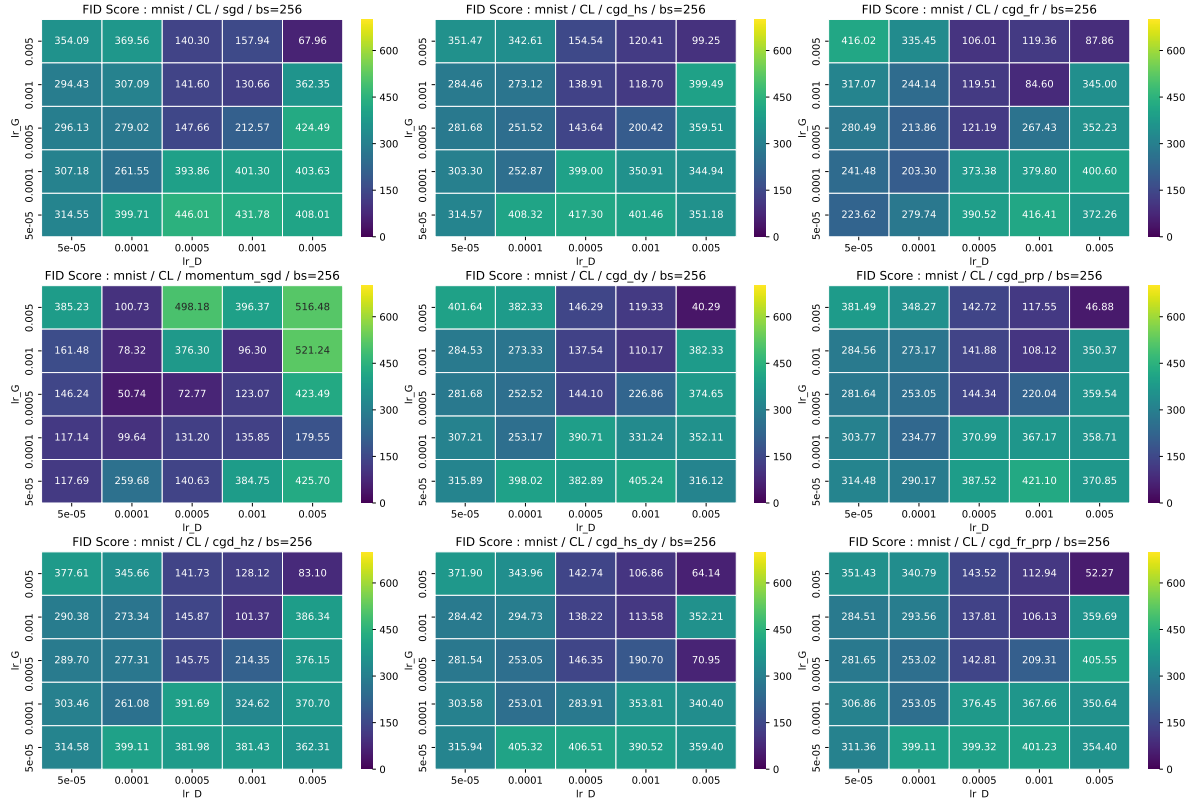


Figure 10. Analysis of the dependence of FID value on LR (MNIST, constant learning rate, batch size = 256): LR of generator on the vertical axis and LR of discriminator on the horizontal axis. The heatmap colors denote the FID scores; the darker the blue, the lower the FID, meaning that the training of the generator succeeded.

E.1.2 Inverse sqrt learning rate

Training was not successful when the inverse sqrt learning rate was used; i.e., FID was large in most cases, and the difference in performance depending on the initial choice of learning rate was smaller than in the constant learning rate case. In the MNIST experiment, the lowest FID scores for momentum SGD were recorded when the learning rate was large.

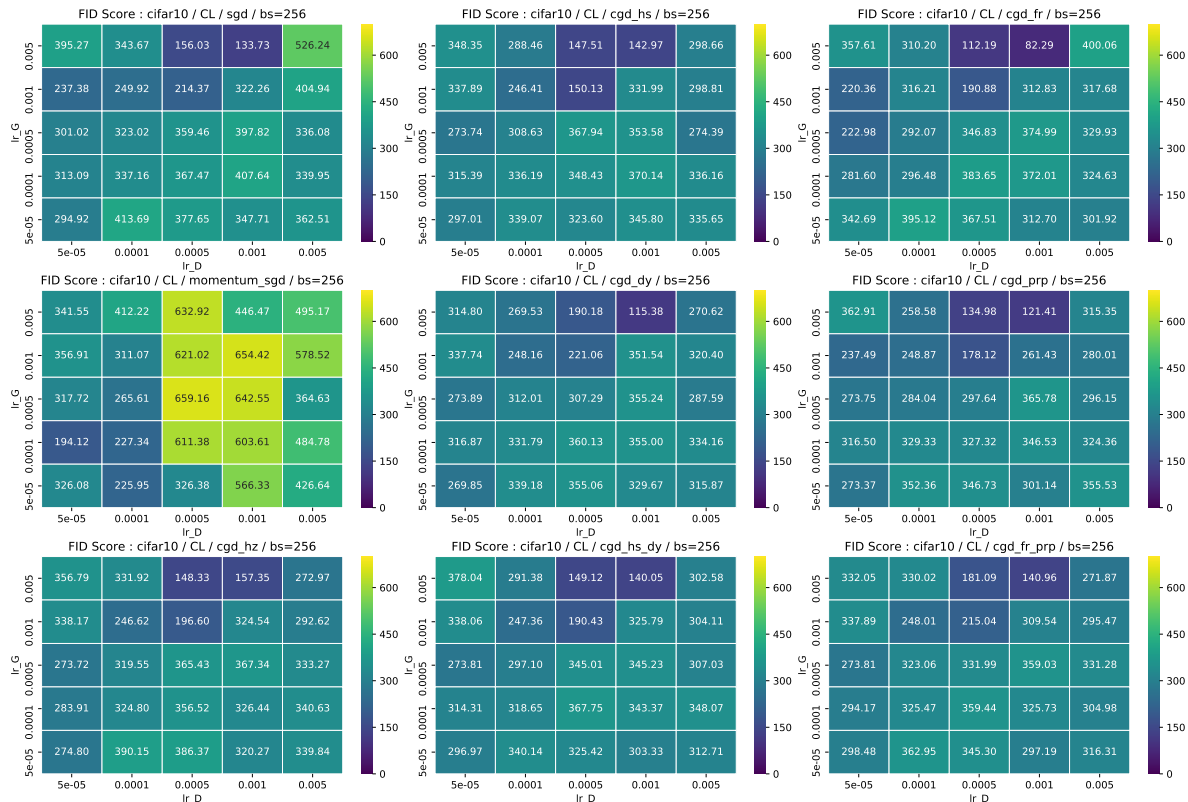


Figure 11. Analysis of the dependence of FID value on LR (CIFAR10, constant learning rate, batch size = 256): LR of generator on the vertical axis and LR of discriminator on the horizontal axis. The heatmap colors denote the FID scores: the darker the blue, the lower the FID, meaning that the training of the generator succeeded.

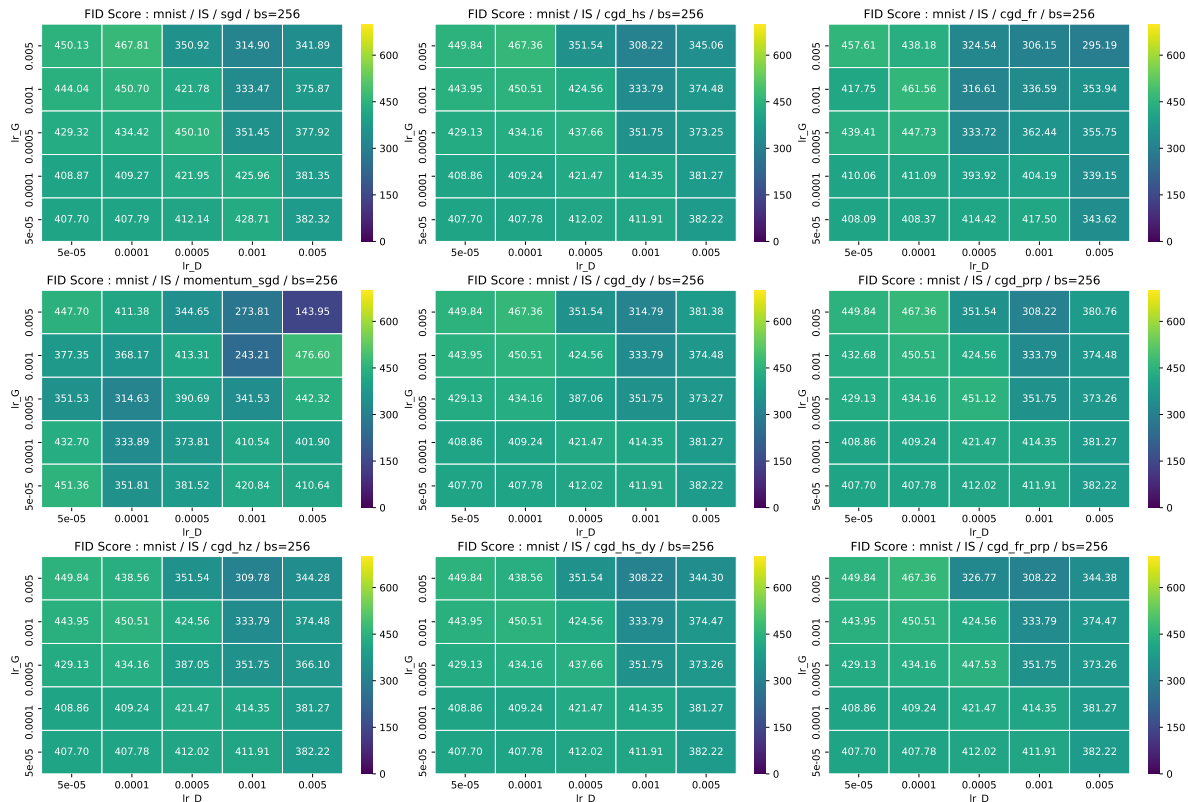


Figure 12. Analysis of the dependence of FID value on LR (MNIST, inverse sqrt learning rate, batch size = 256): LR of generator on the vertical axis and LR of discriminator on the horizontal axis. The heatmap colors denote the FID scores: the darker the blue, the lower the FID, meaning that the training of the generator succeeded.

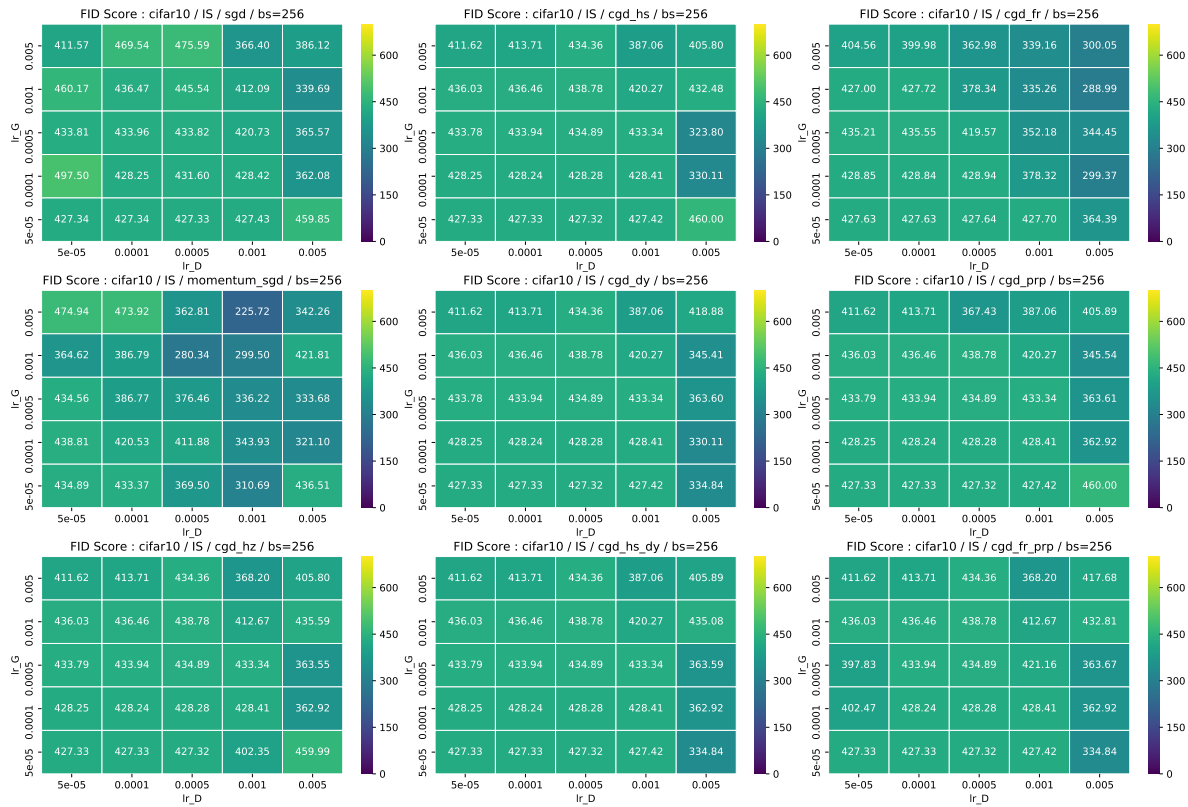


Figure 13. Analysis of the dependence of FID value on LR (CIFAR10, inverse sqrt learning rate, batch size = 256): LR of generator on the vertical axis and LR of discriminator on the horizontal axis. The heatmap colors denote the FID scores: the darker the blue, the lower the FID, meaning that the training of the generator succeeded.